Journal Pre-proof

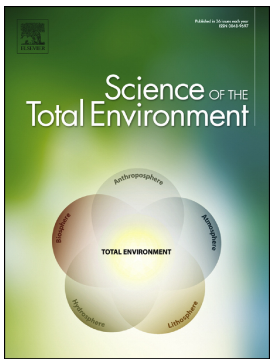

Evaluating tropical drought risk by combining open access gridded vulnerability and hazard data products

Alexandra Nauditt, Kerstin Stahl, Erasmo Rodríguez, Christian Birkel, Rosa Maria Formiga-Johnsson, Kallio Marko, Lars Ribbe, Oscar M. Baez-Villanueva, Joschka Thurner, Hamish Hann

PII: S0048-9697(22)00585-X

DOI: https://doi.org/10.1016/j.scitotenv.2022.153493

Reference: STOTEN 153493

To appear in: *Science of the Total Environment*

Received date: 13 November 2021

Revised date: 25 January 2022

Accepted date: 25 January 2022

Please cite this article as: A. Nauditt, K. Stahl, E. Rodríguez, et al., Evaluating tropical drought risk by combining open access gridded vulnerability and hazard data products, *Science of the Total Environment* (2021), https://doi.org/10.1016/j.scitotenv.2022.153493

This is a PDF file of an article that has undergone enhancements after acceptance, such as the addition of a cover page and metadata, and formatting for readability, but it is not yet the definitive version of record. This version will undergo additional copyediting, typesetting and review before it is published in its final form, but we are providing this version to give early visibility of the article. Please note that, during the production process, errors may be discovered which could affect the content, and all legal disclaimers that apply to the journal pertain.

© 2022 Published by Elsevier B.V.

Evaluating tropical drought risk by combining open access gridded vulnerability and hazard data products

Alexandra Nauditt[1], Kerstin Stahl[2], Erasmo Rodríguez[3], Christian Birkel[4], Rosa Maria Formiga-Johnsson[5], Kallio Marko[6], Lars Ribbe[1], Oscar M. Baez-Villanueva[1,7], Joschka Thurner[1] and Hamish Hann[1]

[1] Institute for Technology and Resources Management in the Tropics and Subtropics, Cologne Technical University of Applied Sciences, Germany

[2] Chair of Environmental Hydrological Systems, University of Freiburg, Germany

[3] Civil and Agricultural Engineering Department, Universidad Nacional de Colombia – Bogotá, Colombia

[4] Department of Geography, University of Costa Rica

[5] Department of Environmental and Sanitary Engineering, State University of Rio de Janeiro (UERJ), Brazil

[6] Department of Built Environment, Aalto University, Finland

[7] Faculty of Spatial Planning, TU Dortmund, Germany

Correspondence to: Alexandra Nauditt, alexandra.nauditt@th-koeln.de, ITT, TH Köln, Robertstr. 2 51105 Köln, Germany

Journal Pre-proof

Abstract

Droughts are causing severe damages to tropical countries worldwide. Although water abundant, their resilience to water shortages during dry periods is often low. As there is little knowledge about tropical drought characteristics, reliable methodologies to evaluate drought risk in data scarce tropical regions are needed.

We combined drought hazard and vulnerability related data to assess drought risk in four rural tropical study regions, the Muriaé basin, Southeast Brazil, the Tempisque-Bebedero basin in Costa Rica, the upper part of the Magdalena basin, Colombia and the Srepok, shared by Cambodia and Vietnam. Drought hazard was analyzed using the variables daily river discharge, precipitation and vegetation condition. Drought vulnerability was assessed based on regionally available socioeconomic data. Besides illustrating the

relative severity of each indicator value, we developed drought risk maps combining hazard and vulnerability for each grid-cell.

While for the Muriaé, our results identified the downstream area as being exposed to severe drought risk, the Tempisque showed highest risk along the major streams and related irrigation systems. Risk hotspots in the Upper Magdalena were found in the central valley and the dryer Southeast and in the Srepok in the agricultural areas of Vietnam and downstream Cambodia. Local scientists and stakeholders have validated our results and we believe that our drought risk assessment methodology for data scarce and rural tropical regions offers a holistic, science based and innovative framework to generate relevant drought related information.

Being applied to other tropical catchments, the approaches described in this article will enable the selection of data sets, indices and their classification - depending on basin size, spatial resolution and seasonality. At its current stage, the outcomes of this study provide relevant information for regional planners and water managers dealing with the control of future drought disasters in tropical regions.

Keywords: Hydrological Drought, Tropics, Satellite data, Hydrostreamer, Vegetation Condition Index, Chirps V2.0

1 Introduction

Droughts are a recurrent phenomenon in tropical regions worldwide (Adamson and Bird, 2010; Erfanian et al., 2017) and are expected to become more severe in the future (Sheffield et al., 2018). Recent El Niño triggered drought disasters occurred in South-East Brazil, January 2014 to December 2015 (Nauditt et al., 2019b; Ribbe et al., 2018), followed by droughts in 2015-2016 affecting Costa Rica (Herrera and Ault, 2017), Colombia (FAO, 2017) and Southeast Asia (Thirumalai et al., 2017), with devastating implications for domestic water supply, agricultural and hydropower production, navigation, fire occurrence and public health (Hoyos et al., 2017). Strong linkages have been found between precipitation patterns and the ENSO phenomenon in the above mentioned regions. El Niño events are associated with decreased rainfalls and droughts over the Amazon, the northeastern parts of South America and the Caribbean (Munoz-Jiménez et al., 2018; Ault 2020; Cai et al., 2020). Hund et al. (2021) found that extreme El Niño events can strongly reduce streamflow and groundwater recharge in seasonally dry river basins. This is also the case for Southeast Asia. Räsänen et al., 2016 found a correlation between reduced precipitation rates and El Niño for Thailand, Cambodia, Vietnam, Myanmar, China and Lao People's Democratic Republic (PDR). Also in

2015-2016, the Mekong basin was impacted by the El Niño, with high rainfall deficits over the sub-basins in Laos and Cambodia (Ruiz-Barradas & Nigam, 2018).

Rural areas that rely on rain-fed agriculture, livestock and milk production, were extremely impacted due to the lack of water storage or distribution infrastructure (Nauditt et al., 2019a). To avoid such economic losses during future drought events, the respective governments have been seeking for more effective adaptation strategies (IDEAM et al., 2014; Emater-RIO et al. 2016; FAO, 2017; UNGRD et al., 2018). Decisions related to drought adaptation, though, need to rely on a profound knowledge about drought hazard, vulnerability and exposure; spatially varying risk information that is rarely available in data scarce tropical regions.

Many concepts have been developed to evaluate drought risk, each varying in its definition and interpretation of the terms “risk”, “hazard”, “vulnerability” and “exposure” (Carrão et al., 2016; Stahl et al., 2016; Vogt et al., 2018; Naumann et al., 2019; Meza et al., 2019). “Vulnerability” definitions and concepts are particularly diverse, as they may consider a large variety of economic assets, human conditions and environmental characteristics (De Stefano et al., 2015; González-Tánago et al., 2015; Naumann et al., 2018; Hagenlocher et al., 2019).

Nonetheless, although varying in terminology, there is a wide agreement that risk cannot be understood by looking only at either climate anomalies or only at socioeconomic vulnerability factors (UN-ISDR, 2009; Bachmair et al., 2017). Understanding risk requires a more holistic evaluation of different conditions leading to drought disasters: What extent and duration of a hydro-climatic deficiency caused drought impacts at which location? How did the catchment, vegetation and discharge respond to this extreme event? Which environmental and economic sectors were affected? Since such characteristics are climate, region- and sector specific, there is a demand to design locally suitable drought risk assessment approaches and related data sets (Naumann et al., 2019).

The scale of analysis matters. Widely applied monthly scale standardized indices (eg. SPI 12) are useful for large scale drought risk assessment (Naumann et al., 2018; Vogt et al., 2018). Tropical climates are often dominated by a strong seasonality and a topography-influenced spatial rainfall variability. Few days without precipitation might lead to a water deficit that can affect livestock grazing and rain-fed agricultural production. Indices based on monthly hydro-meteorological values might not detect short-term deficits in quickly responding catchments. For tropical regions, it has therefore been proven useful to assess meteorological and hydrological drought hazard at a daily timescale (Nauditt et al., 2017; Firoz et al.,

2018). Also the spatial distribution and coverage of hydro-climatic observations used to detect drought anomalies are of key importance for hazard assessment. During drought, topography, geology, soil and land-cover catchment characteristics as well as human water interventions influence hydrological processes, catchment storage and release and therefore play a major role in the evolution of low flows (Bruijnzeel, 2004; Calder et al., 2007; Birkel et al., 2012; Stoelzle et al., 2014; van Loon and Laaha, 2015; Van Loon et al., 2016). Altogether these influences cause a strong variability of climatic and hydrological drought hazard in tropical space (Nauditt et al., 2019b).

Daily time step data, needed to effectively evaluate drought hazard in tropical catchments, are rarely available. Sheffield et al. (2018) highlight the potential of satellite remote sensing and reanalysis data products to improve water resources management in regions with sparse in-situ monitoring networks. Open access high resolution remote sensing data products are continuously increasing in quantity (AghaKouchak et al., 2015; Mariano et al., 2018). In this context, a variety of gridded datasets are available, including daily precipitation (Funk et al., 2015; Baez-Villanueva et al., 2018&2020), surface water (Beck et al., 2016), groundwater (Thomas et al., 2014), reservoirs (AghaKouchak et al., 2018), soil moisture (Samaniego et al., 2018; Tijdeman and Menzel, 2020), and vegetation (Pinzón and Tucker, 2014; Nguyen et al., 2019). Especially vegetation condition indices like fAPAR, NDVI, EVI and VCI play an increasing role for drought monitoring and research in data scarce regions. They can provide spatially distributed information on soil and vegetation moisture anomalies on the ground (Heydari et al., 2018; Recuero et al., 2019) that is not dependent on sparsely monitored hydro-climatic data.

Exposure and vulnerability information are also sparse, especially in rural tropical regions. Vulnerability evaluation should be ideally based on historical drought impact data (Stahl et al., 2016; Bachmair et al., 2016; Blauhut et al., 2016), but these are usually not systematically monitored and recorded; rare examples being the US Drought Impact Reporter (droughtreporter.unl.edu) , the European Drought Impact Database (Stahl et al., 2016) or observer-based systems such as the Czech INTERSUCHO (www.intersucho.cz). Alternatively, vulnerability data is often replaced by exposure related information (Carrão et al., 2016; Naumann et al., 2018; Vogt et al., 2018; Naumann et al., 2019), that is available as gridded socioeconomic data sets showing the spatial distribution of population-, livestock- and crop densities as well as socio-economic, demographic and infrastructural characteristics. Such remote sensing and gridded data-based drought risk assessment approaches have often been carried out at global or

regional scale (Carrão et al., 2016; Hagenlocher et al., 2019), but have rarely been applied to local and catchment scale drought risk. This study evaluates the performance of gridded datasets related to hydro-climatic and socio-economic information to derive relevant drought risk information for catchments of different sizes (between 5 450 and 49 382 km²) and differing tropical climates.

In line with the above, **the overall aim** of this study is to identify and characterize drought risk hotspots in rural and data scarce tropical regions as a basis for drought management.

Specific objectives:

- to identify the spatially distributed cumulative duration of hydrological and meteorological drought hazard
- to understand spatially varying and sector related drought vulnerability
- to visualize spatial distribution of drought risk in four tropical catchments that vary in size, topography, climate and water infrastructure development
- to attribute the relative spatial contribution of hazard and vulnerability related factors to drought risk

Journal Pre-proof

2 Study regions and data sets

2.1 Study regions

We selected four rural catchments in tropical regions that were affected by severe drought disasters during the last decade. South-Eastern Brazil was hit by a long term drought from January 2014 to December 2015 (Nauditt et al., 2019b; Ribbe et al., 2018). The El Niño event in 2014-2016 also caused droughts in Northern Costa Rica (Herrera and Ault, 2017) and the Magdalena Basin in Colombia (FAO, 2017; Vega-Viviescas and Rodríguez, 2019) and Southeast Asia (Thirumalai et al., 2017). Figure 1 gives an overview on the characteristics of the four *study regions*, each differing in size, topography, seasonality and level of human intervention.

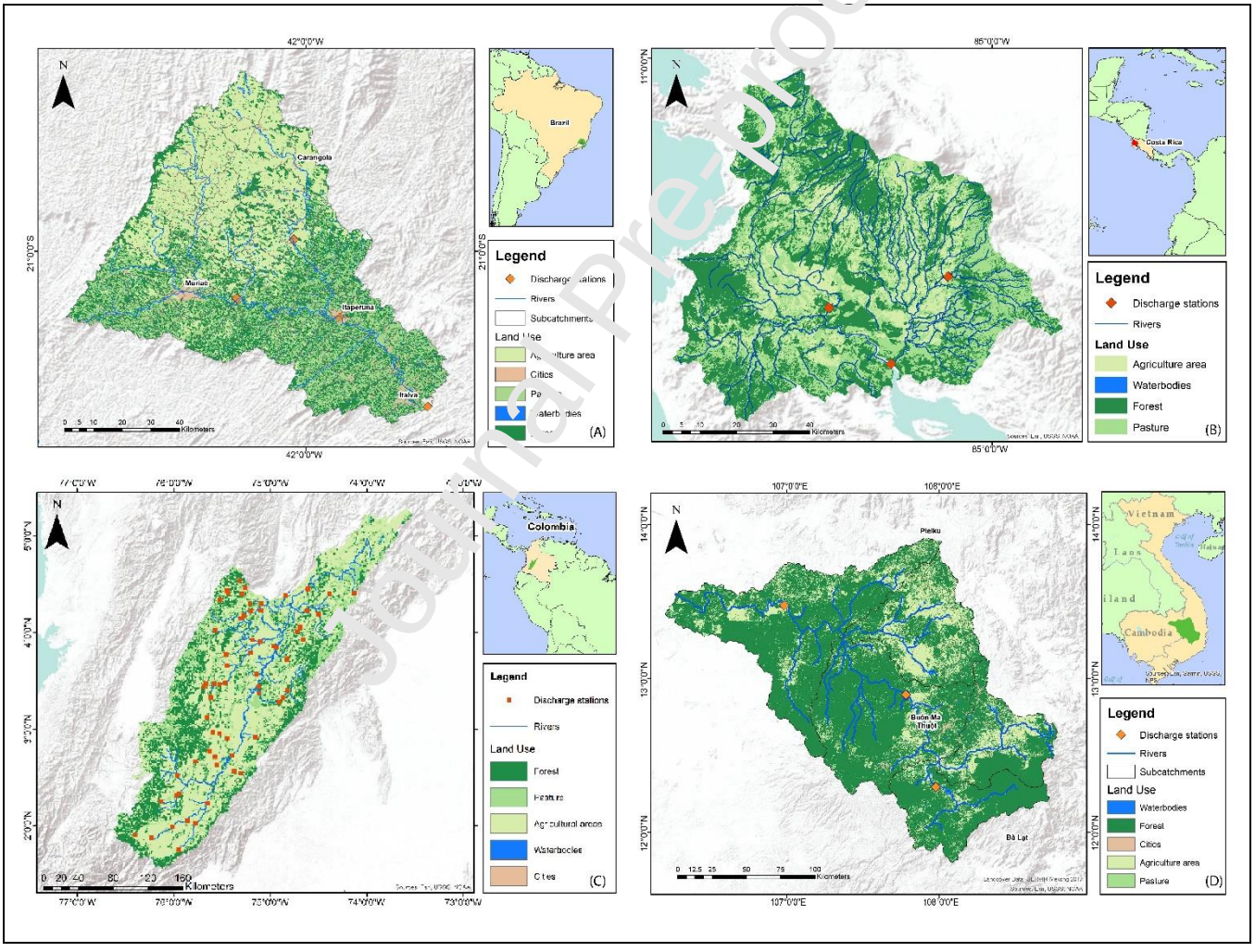

Figure 1. *Study regions: river network, discharge stations, major land uses and urban areas of the (A) Muriaé, subbasin of the Paraíba do Sul in South Eastern Brazil, (B) the Tempisque basin in North Costa Rica, (C) the Upper Magdalena basin in Colombia and (D) the Srepok basin in the Lower Mekong shared by Cambodia and Vietnam***.**

Table 1: Basin characteristics of the four study regions

	The Muriaé basin, South Eastern Brazil	The Tempisque-Bebedero basin, Costa Rica	The Upper Magdalena basin, Colombia	The Srepok basin, Cambodia and Vietnam
Size:	7 220 km²	5 455 km²	49 382 km²	30 900 km²
Elevation:	10 to 2 000 m.a.sl.	0 to 1 916 m.a.sl.	222 to 3 685 m.a.sl.	66 to 2 283 m.a.sl.
Precipitation:	1 000–2 000 mm.	1 000-3 000 mm.	2 500-3 000 mm	1 569–2 800 mm
Mean annual discharge:	118 m³/s.	Tempisque 27 m³/s; Bebedero 10 m³/s.	1 330 m³/s	634.2 m^3/s. (Constable, 2015)
Total population:	ca. 100 000 inhabitants	ca. 382 900 inhabitants.	ca. 1.5 million inhabitants	ca. 2.9 million inhabitants
Climate: (Peel et al., 2007)	Tropical savanna climate (Aw), dry-winter humid subtropical climate (Cwa) and Dry-winter subtropical highland climate (Cwb).	Tropical savanna climate (Aw).	Tropical rainforest climate (Af), tropical monsoon climate (Am), oceanic climate (Cfb), and tropical savanna climate (Aw).	Tropical savanna climate (Aw) and tropical monsoon climate (Am).
Major land uses: (Arino et al., 2012)	68.3 % pasture, 24.1 % forest, 7 % agriculture and 0.6 % urban.	17 % pasture, 5 % forest, 76 % agriculture and 2 % urban.	38 % agricultural area, 51 % forest, 9 % pasture and 1 % urban areas.	40 % pasture, 34.5 % forest, 24.9 % agriculture and 1 % urban.

Journal Pre-proof

2.2 Data

2.2.1 Discharge data set: Hydrostreamer v1.0

Available discharge observations data in the study regions (Figure 1) do not allow to display the spatial variability in hydrological behaviour. We applied a state of the art downscaling tool Hydrostreamer (Kallio, 2020) to the spatially coarse global discharge data product from the ISIMIP 2a (Gosling et al., 2017) experiment. Downscaling is carried out by areal interpolation, where the source runoff data are distributed

to intersecting higher-resolution catchments, routed downstream, and optimized against observed streamflow (see detailed description in Kallio et al., 2019&2021.

Available daily discharge observations were used to validate and optimize the Hydrostreamer results. For the Muriaé, five daily discharge time series were obtained by the National Water Agency of Brazil (ANA, 2019; Nauditt et al., 2019a; Nauditt et al., 2019b). For the Tempisque, data from two discharge stations were acquired by the Hydrological Department of the Electricity Institute of Costa Rica ICE (2019) 1980-2003 and for the period 2003-2018 by the Institute for Aqueducts and Sanitation (AYA, 2019). For the Upper Magdalena, we obtained daily time series from 46 discharge stations from IDEAM (2019) and for the Srepok, daily data from three discharge stations (Kallio et al., 2019; Kallio, 2020; MRC, 2018) were used.

2.2.2 Precipitation

Observation data that were used to evaluate precipitation products for the Magdalena and the Muriaé are described in Baez-Villanueva et al. (2018), for the Srepok in Dandridge et al. (2019) and for the Tempisque in Venegas-Cordero et al. (2020). We selected the gridded daily precipitation dataset CHIRPS v2.0 (Funk et al., 2015), which has a spatial resolution of 0.05° for the period 1981-2018 after evaluating available precipitation products in a point to pixel analysis (Baez-Villanueva et al., 2018; Dandridge et al, 2019) and in hydrological modelling (Nauditt et al., 2019b).

CHIRPS v2.0 showed a good goodness-of fit (GOF) performance during point to pixel evaluation and HBV rainfall runoff modelling (Baez-Villanueva et al., 2018; Nauditt et al., 2019b; Venegas-Cordero et al., 2020). Additionally, CHIRPS v2.0 covers the longest time period (1981 to date) and has a higher spatial resolution compared to other available precipitation products.

2.2.3 Vegetation Condition

To understand the spatial variation of drought related vegetation condition, we used MODIS MOD13Q13 (2000-2017) 16-day composite NDVI imagery at 250 m resolution. We identified the driest month in record (1981-2018) applying the Standardized Precipitation Index (SPI) (McKee et al., 1993) to CHIRPS v2.0 (Nauditt et al., 2019b).

2.2.4 Vulnerability

We evaluated gridded data sets in terms of their suitability to represent vulnerability and selected the following data sets available for all our study regions:

Table 2: Vulnerability related data sets

Data set	Measure	Source	Resolution
Gridded Livestock of the World	livestock density	(Robinson et al., 2014)	5 km
Global Agricultural Lands 2000	cropland density	(Ramankutty et al., 2008)	1 km
GHS Population Grid 2015	population density	(EU-JRC, CIESEN, 2015)	250 m
Major roads 2013	Proximity to infrastructure	(CIESIN, 1997-2020)	30 m
Global GDP PPP/HDI 2015	Total GDP per grid cell	(Kummu et al., 2018)	1 km

Journal Pre-proof

3 Methodology

3.1 Drought Risk Assessment

Figure 2 illustrates the overall methodology applied in this study. We evaluate drought risk as a combination of hazard and vulnerability:

$$\boldsymbol{dr_i} = \frac{dh_i + dv_i}{2} \qquad (1)$$

Where dr represents drought risk, dh drought hazard, dv drought vulnerability and i grid cell.

Hazard (dh_i) is defined by drought in meteorological, hydrological and vegetation condition indices.

Vulnerability (dv_i) is defined as the potential of a drought to cause damages in selected socioeconomic sectors using typical exposure information.

We used two groups of variables (hydro-climatic and socio-economic) and calculated index values for each grid-cell (*i*) for each variable. All layers were resampled to a spatial resolution of 30 m using bilinear interpolation of the nearest neighbor method. The resulting values were then equally weighted to obtain maps for each index, hazard, vulnerability and risk. More details about the methodological process are given in sections *3.2* and *3.3.*

Journal Pre-proof

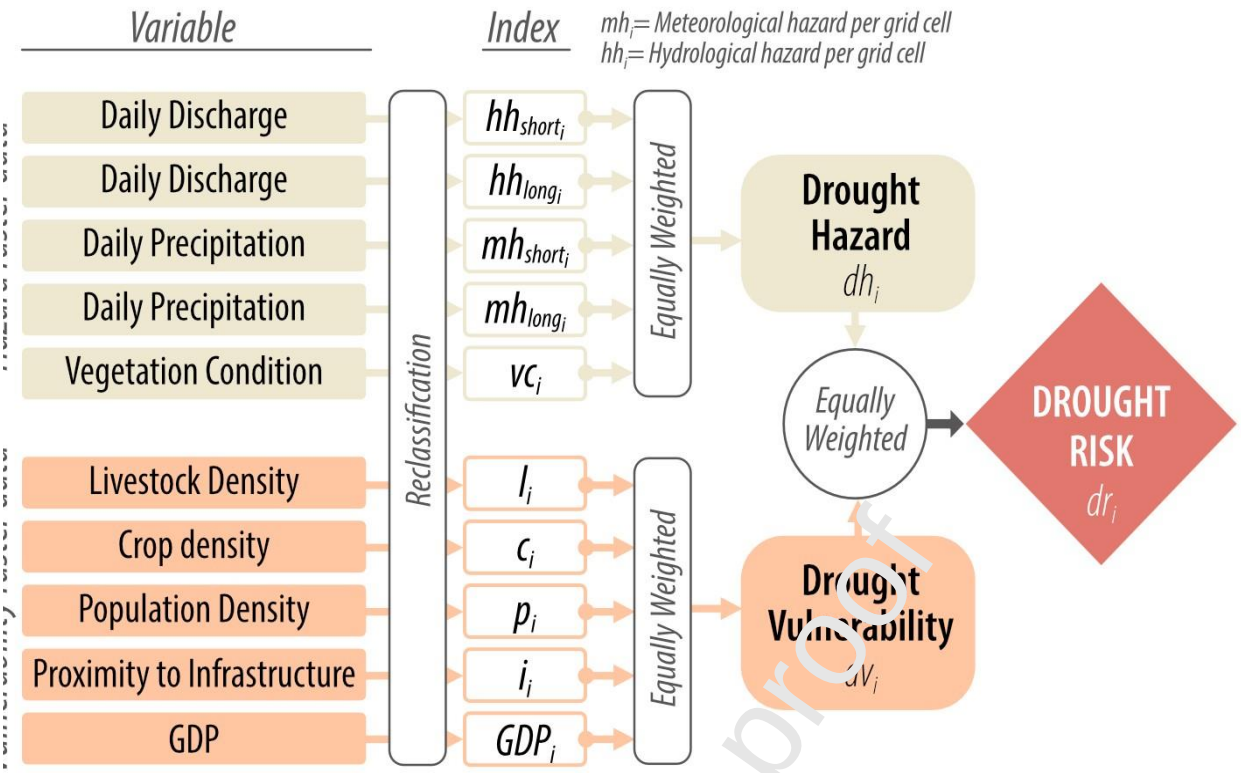

Figure 2: *Overall drought risk assessment methodology showing the input variables, related Indices and output variables.*

Journal Pre-proof

3.2 Drought Hazard

3.2.1 Hydrological Drought Index

To obtain daily scale **hydrological drought** signals, we applied the widely used threshold method (e.g. Tallaksen, 2000) using a daily varying Q_{95} threshold (Fleig et al., 2006; WMO, 2008). We selected the period 2000-2015 that corresponds to the record length of CHIRPS v2.0 data. We defined more or equal than 12 days below a daily varying Q_{95} threshold as a **long** hydrological tropical drought event (hh_{long}) and 5-11 days below that threshold as a **short** hydrological tropical drought event (hh_{short}). We used pooling to remove single days when streamflow went above the threshold by less than 20 %. Resulting short and long hydrological drought indices (hh_i) were derived as the cumulative drought duration of events for each grid-cell. So (hh_{short_i}) is the sum of all short-duration (5-11 days) events and (hh_{long_i}) is the sum of long-duration (>=12 days) events. The cumulative duration of detected events was classified into five severity categories (*Sc*). More than 75 short drought events during the period of 37 years were classified as the most severe short drought hazard and more than 50 events with more or equal than 12 days below Q_{95} were considered the most severe long drought hazard (*Sc* 5) (Table 3).

3.2.2 Meteorological Drought Index

The **meteorological drought** index (mh_i) evaluates the cumulative drought duration of precipitation drought events. To represent long and short meteorological drought events in tropical regions, we defined two classes of drought intensity for precipitation deficits: >= 20 days with rainfall below 0.3 mm as a long meteorological drought: (mh_{long}) and 5-19 days as a short meteorological drought: (mh_{short}) with rainfall below 0.3 mm. The number of detected events were classified into 5 severity categories (Table 3)

3.2.3 Vegetation Condition Index

The **vegetation condition** related drought hazard *vc* is represented by the vegetation condition in the driest month in record. We identified the driest month in record using the SPI. To understand the spatial variation of vegetation condition, we used the Vegetation Condition Index (VCI) (Kogan, 1995; Quiring and Ganesh, 2010; Dutta et al., 2016) applied to NDVI imagery. We decided to use the VCI due to the following reasons: *(i)* VCI excludes the variable temperature and related evaporative demand. In other indices, Land Surface temperature (LST) and the normalized difference vegetation index (NDVI) inversely vary over time (i.e., there is a negative NDVI-LST correlation) (Karnieli et al., 2010). *(ii)* Under drought periods, LST is

expected to be high, while NDVI is expected to be low compared to normal conditions. However, past studies have shown that there are often positive NDVI-LST correlations over the tropics and high latitudes, which represent areas where vegetation growth is energy limited (Nemani et al. 2003; Julien and Sobrino 2009). *(iii)* In the Tropics, increased temperatures may lead to increased plant biomass as confirmed by several studies through warming experiments (Van Wijk et al. 2003; Stow et al. 2004; Walker et al. 2006). We therefore decided to use VCI, which we consider suitable to detect vegetation related drought anomalies in the tropics, especially in tropical grassland ecosystems.

The vegetation related drought index (vc_i) was established by inversely rating VCI values for each grid-cell. In contrast to the hydrological and meteorological indices, vc_i has a negative correlation with drought severity. Values between 50 % and 100 % indicate moisture rich vegetation conditions, values between 50 % and 35 % short drought conditions and values below 35 % long drought conditions (Kogan, 1995). The detailed methodology is described in Nauditt et al., 2019b. VCI percentage values were classified into five severity categories (Table 3).

3.2.4 Drought Hazard Index

The overall drought hazard (*dh)* for each grid-cell *(i)* is calculated by the equally weighted severity class (*Sc)* values (Table 3) of each hazard index as:

$$\boldsymbol{dh}_i = \frac{S_c\left(hh_{short_i}\right)+S_c\left(hh_{long_i}\right)+S_c\left(mh_{Short_i}\right)+S_c\left(mh_{long_i}\right)+S_c(vc_i)}{5} \quad (2)$$

Where *dh* is the drought hazard, *i* the location (grid cell) and *Sc* the severity class. hh_{short_i} represents the cumulative duration of short hydrological drought events based on number of events, hh_{long_i} the cumulative duration of long hydrological drought events, mh_{short_i} the cumulative duration of short meteorological drought events, mh_{long_i} the cumulative duration of long hydrological drought events and vc_i the vegetation condition related hazard (Table 3).

Table 3: Hazard indices, their severity classification and allocation to five severity classes (Sc):

Drought	$\boldsymbol{hh_{short_i}}$	$\boldsymbol{hh_{long_i}}$	$\boldsymbol{mh_{short_i}}$	$\boldsymbol{mh_{long_i}}$	$\boldsymbol{vc_i}$

Hazard Index	Number of drought events with 5-11 days below Q_{95} daily variable threshold	Number of drought events with >=12 days below Q_{95} daily variable threshold	Number of drought events with 5-19 days below 0.3 mm of precipitation	Number of drought events with >=20 days below 0.3 mm of precipitation	Vegetation Condition Index (VCI) value (%) for the driest month in records (SPI12)
Severity class (Sc)	***Classification***				
1	0-30	0-25	0-30	0-25	> 50
2	30–45	25–32	30–45	25–32	40-50
3	45–60	32–40	45–60	32–40	30-40
4	60–75	40–50	60-75	40–50	20-30
5	> 75	> 50	> 75	> 50	0-20

3.2.5 Drought Vulnerability

Due to missing information on drought impacts, sensitivity, adaptive capacity or other potential constituents of vulnerability, we used exposure data as proxies for vulnerability. This approach corresponds to the concept of IPCC 2014, where vulnerability is described as a combination of exposure, sensitivity and adaptive capacity, while risk is understood as a combination of vulnerability and hazard (IPCC, 2014). We used open access gridded datasets for five socioeconomic exposure related variables to represent spatial drought vulnerability in the four study regions. All datasets were resampled to a 30 m resolution using the nearest neighbor method to account for differences in grid cell resolution. Each data set was reclassified and given a rating based on positive or negative correlation to vulnerability. The overall drought vulnerability *dv* for each grid cell $_i$ is calculated by the equally weighted severity class *Sc* values (Table 4) of each vulnerability index as:

$$\boldsymbol{dv}_i = \frac{S_c(l_i) + S_c(c_i) + S_c(p_i) + S_c(i_i) + S_c(GDP_i)}{5} \quad (3)$$

Where dv_i *is* overall drought vulnerability per grid-cell, *Sc* the severity class, l_i the livestock density index, c_i the crop density index, p_i the population density index, i_i the index for proximity to infrastructure and GDP_i the GDP index per grid-cell. Table 4 gives an overview on the severity classification for each index.

Table 4: Vulnerability indices, *their severity classification and allocation to five severity classes*

Vulnerability index	l_i Livestock density (head per km^2)	c_i Cropland (% area)	p_i Population Density (persons/grid cell)	i_i Proximity to Infrastructure (m)	GDP_i (Million USD PPP per km²) for reference year 2011
Severity class	***Classification***				
1	0-15	0-0.1	0-50	0-100	>20
2	15-30	0.1-0.2	50-100	100-250	5-20
3	30-40	0.2-0.3	100-250	250-500	2-5
4	40-50	0.3-0.4	250-500	500-1000	1-2
5	>50	>0.4	>500	> 1000	0-1
Correlation	positive	positive	positive	positive	negative

Journal Pre-proof

4 Results

4.1 Drought hazard (dh_i), drought vulnerability (dv_i) and drought risk (dr_i) for each grid-cell $_i$ in the four study regions

Figure 3 gives an overview on spatial coverage (% of grid-cells) of drought hazard, vulnerability and risk in the four study regions. Due to the equal weighting of the individual hazard and vulnerability severity values, the percentages of basin area in the severity classes (*Sc*) 1 and 5 are small. Therefore, severity class *Sc 4* can be considered as most severe and *Sc 2* as least severe.

For the **Muriaé**, results suggest severe drought vulnerability (dv_i) in most of the area with 73.1 % in *Sc* 4 and 26.2 % in *Sc* 3. Drought hazard (*dh*) was found in *Sc* 3 with 57.4 % and *Sc* 2 with 24.4 % of the Muriaé basin. The **Tempisque** showed hazard (*dh*) with 25.7 % of the area in *Sc* 4, 0.7 % in *Sc* 5 and 56.5 % in *Sc* 3, while percentage of area exposed to drought vulnerability (*dv*) is largest in *Sc* 3 with 81.8 % and 14.2 % in *Sc* 2. **Upper Magdalena** shows vulnerability (*dv*) with 43.1 % in *Sc* 4 and 55 % in *Sc* 3. Results identify hazard (*dh*) with most values in *Sc* 2 with 52 % and 41.3 % in *Sc* 3. Finally, for the **Srepok,** higher hazard (*dh*) was found compared to *dv*, with 38.5 % in *Sc* 4 and 54 % in *Sc* 3 of its basin area, while vulnerability is highest in *Sc* 3 with 87.4 % and 8.9 % in *Sc* 2 (Figure 3).

Journal Pre-proof

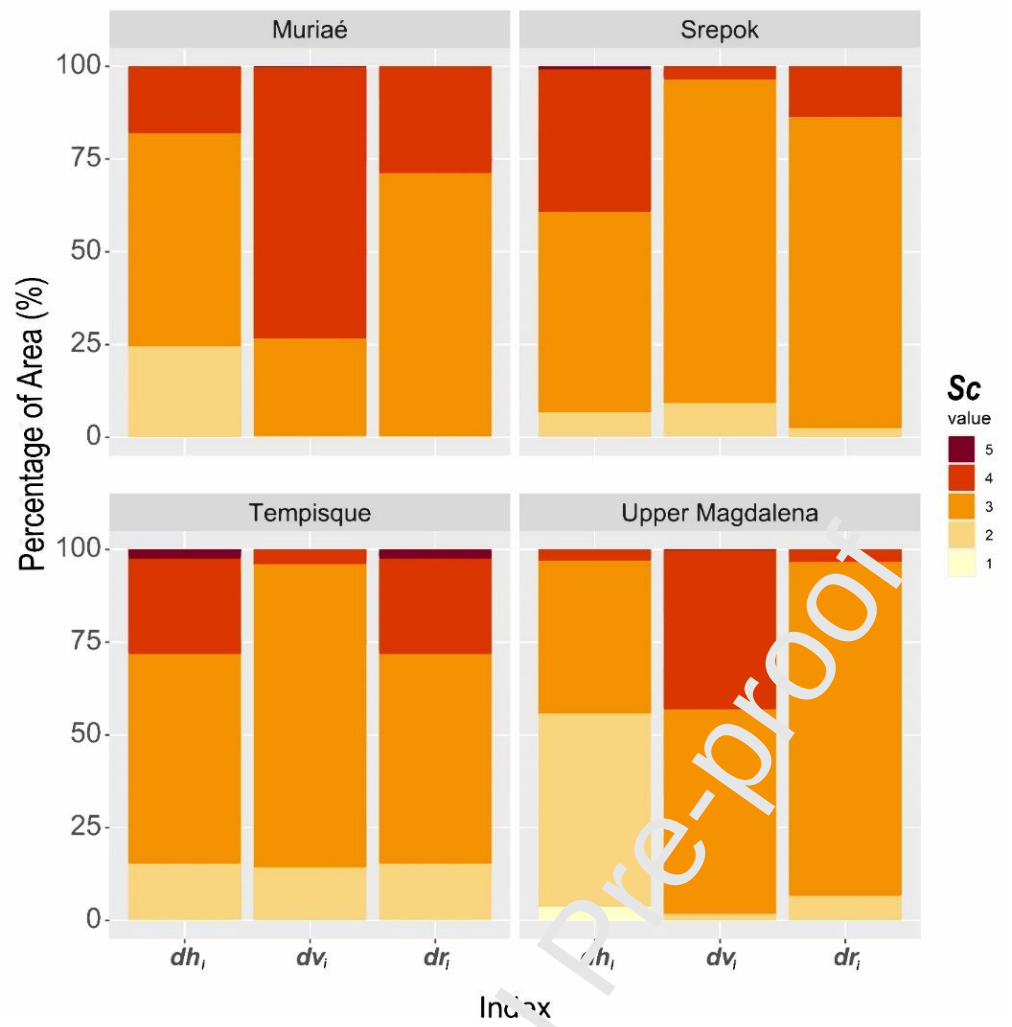

Figure 3: Severity class (*Sc*) distribution per percentage of area for drought hazard (*dh*), vulnerability (*dv*) and risk (*dr*) in the four study regions

Figure 4 shows balloon plots indicating the percentage of the basin area covered by the severity classes (*Sc*)1-5 for each drought index. All study regions show a high vulnerability related to low GDP (*Sc* 5) and a low vulnerability (*Sc* 1) related to population density (p_i).

For the **Muriaé,** the highest severity was found for livestock (l_i) (with 78 % in *Sc* 5) and crop density (c_i) (33.2 % in *Sc* 5 and 31.1 % in *Sc* 4) as well as for proximity to infrastructure (i_i) (43.5 % in *Sc* 5 and 25.7 % in *Sc* 4). The remaining indices showed a nearly homogenous distribution across the severity classes.

For the **Tempisque**, the results show highest values for short hydrological drought hazard ($\boldsymbol{hh_{short_i}}$) with 42 % of its area in *Sc* 4 and 10,5 % in *Sc* 5, for $\boldsymbol{mh_{short_i}}$ with 33 % of its area in *Sc* 4 and 26 % in *Sc* 5 and for $\boldsymbol{hh_{long_i}}$ with 23 % of its area in *Sc* 5. Lower values were shown for the vulnerability indices proximity to infrastructure l_i with 25.1 % of area in *Sc* 4 and 19.1 % in *Sc* 5 and Crop density c_i (44.2 % of area in *Sc* 4 and 17 % in *Sc* 5) (Figure 4).

Journal Pre-proof

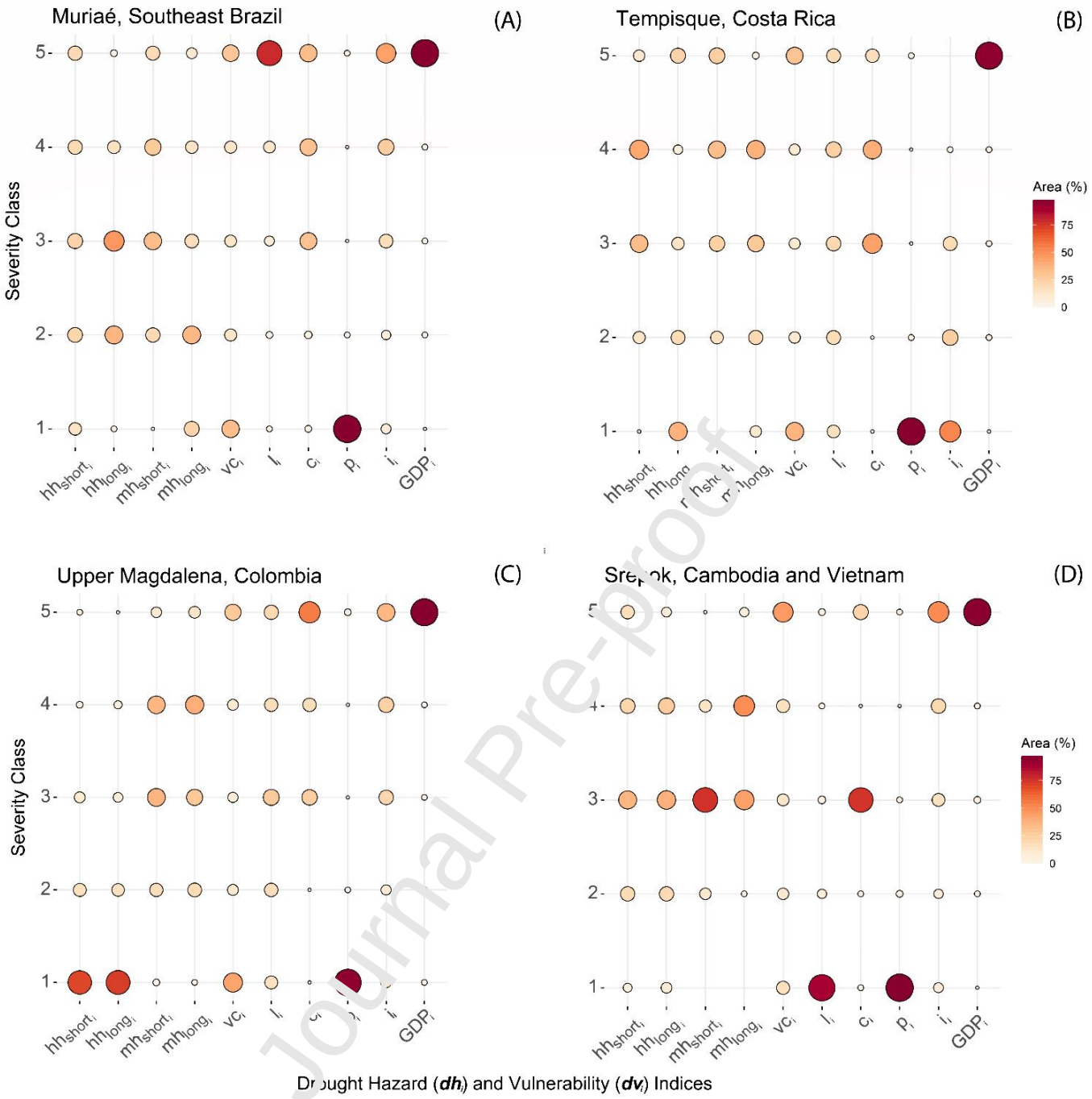

Figure 4: Drought hazard and vulnerability indicator values distributed to percentage of catchment area in the four study regions

For the **Upper Magdalena,** highest severity was found for vulnerability indices crop density (c_i) (55.6 % in *Sc 5* and 18.1 in *Sc 4*), livestock density (l_i) (21.4% in *Sc* 5 and 16.7 *%* in *Sc 4)* and proximity to infrastructure (36.2 % in *Sc* 5 and 24.8 *% in Sc* 4). Lower values for hazard were found for mh_{short_i} with 37 % in *Sc* 3 and 35.8 % in *Sc* 4, for mh_{long_i} (11. 6 % in *Sc* 5 and *39.2 %* in *Sc* 4*)* and very low values for hh_{long_i} (73.9 % in *Sc* 1 and *15.4 %* in *Sc* 2*) and* hh_{short_i} (71.8 % in *Sc* 1 and *17.2 %* in *Sc* 2*).*

For the **Srepok**, results show highest values for vegetation condition related condition hazard vc_i (46.4 % in *Sc* 5 and 15.9 % in *Sc* 4), followed by meteorological drought hazard mh_{long_i} (*50.1 %* in *Sc* 4 and 5.8 % in *Sc* 4*).* The other hazard indices resulted in values distributed across the *Scs*. Highest vulnerability was found for proximity to infrastructure (i_i) with 51.5 % in *Sc* 5 and 20.6 % in *Sc* 4. The remaining vulnerability indices showed low values as for livestock density (l_i) 88.2 % in *Sc* 1 and for crop density (c_i) 75.4 % in *Sc* 3.

4.2 Spatial distribution of drought hazard (dh_i) in the four study regions

Figure 5 illustrates the weighted drought hazard based on the meteorological, hydrological and vegetation condition-based indices for each grid cell in the four study regions. Red corresponds to *Sc* 5 and green to *Sc* 1. For the **Muriaé**, drought hazard was found to be highest in the Southwestern downstream part due to the larger share of *Sc* values for hh_{short_i}, mh_{long_i} and vc_i (see individual maps in the supplementary material).

For the **Tempisque** basin, drought hazard was found to be highest in the downstream part in the North over the river estuary and for the Eastern part along the main Tempisque River stretches and the Bebedero tributary upstream (Figure 5). Duration of periods without rainfall and resulting vegetation moisture loss were stronger in the Eastern part of the basin.

For the Southwestern upstream area of the **Upper Magdalena** basin in Colombia, the results show strongest hazard values in the Southeastern upstream part where most meteorological drought periods and also vegetation related anomalies were detected and along the main Magdalena river due to hydrological droughts. For the **Srepok** basin, the strongest hazard values were observed in the Southeastern upstream region over the Vietnamese highlands and the Cambodian North and Northwestern downstream region due to high vegetation condition hazard v_i and hh_{long_i} (Figure 5). Detailed results for each layer are given in the supplementary materials.

Journal Pre-proof

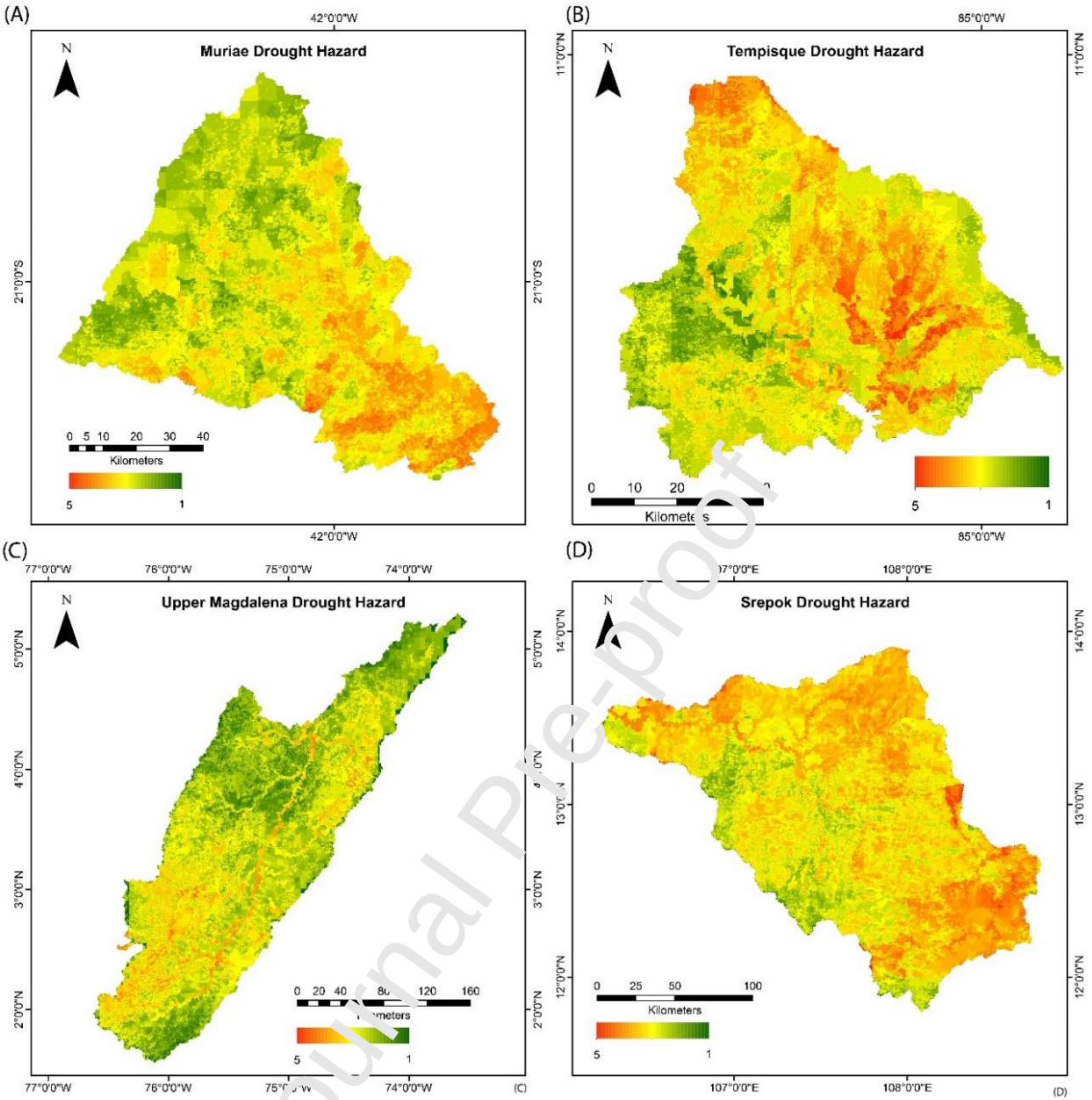

Figure 5: Map of severity class values for spatially distributed drought hazard (dh) found in the four study regions

4.3 Spatial distribution of drought vulnerability

Figure 6 shows the spatial distribution of drought vulnerability in the four study regions. For the **Muriaé**, the data evaluation suggests a strong vulnerability all over the region due to high cropland and livestock density, low GDP of the rural population and long distances to infrastructure - except along the major roads where the indicators for crop density and proximity to infrastructure show low values. Results for the **Tempisque** show a high vulnerability almost all over the place as cropland and livestock pasture is strongly

developed. Only the protected areas in the forested Northwestern and Central regions show lower vulnerability values. Similarly, for the **Upper Magdalena** drought vulnerability was found almost everywhere, despite the Southwest, where protected areas are located. The **Srepok shows** less vulnerability severity, with main regions located in the Vietnamese Southeastern upstream part, the Northeaster Cambodian part and the Northwestern downstream area (Figure 6). Detailed results for each layer are presented in the supplementary materials.

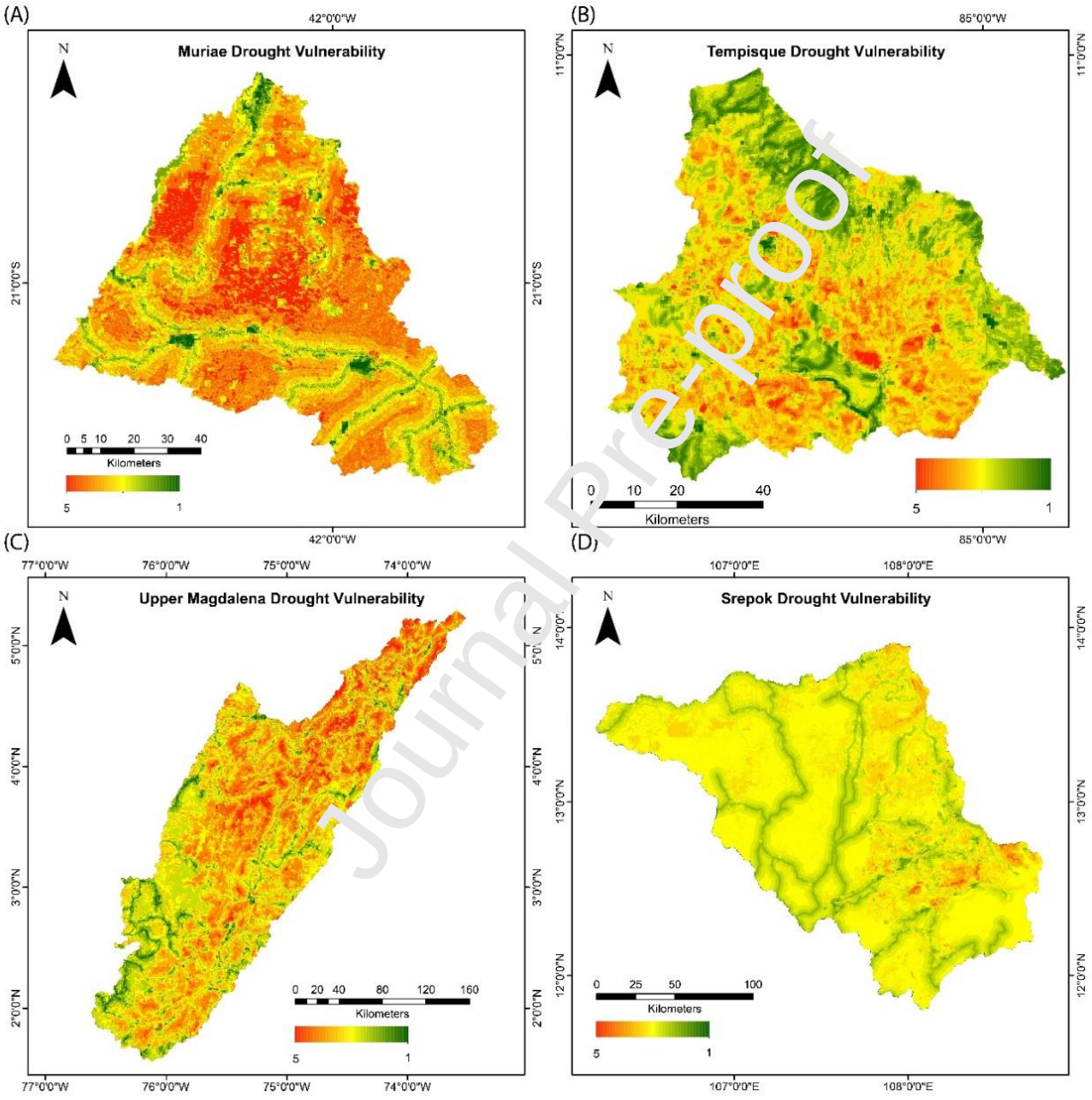

Figure 6: Map of severity class values for spatially distributed drought vulnerability (*dv*) found in the four study regions

Journal Pre-proof

4.4 Drought risk

Figure 7 illustrates the spatial distribution of drought risk (*dr*) in the four study regions based on equally weighted hazard and vulnerability severity values.

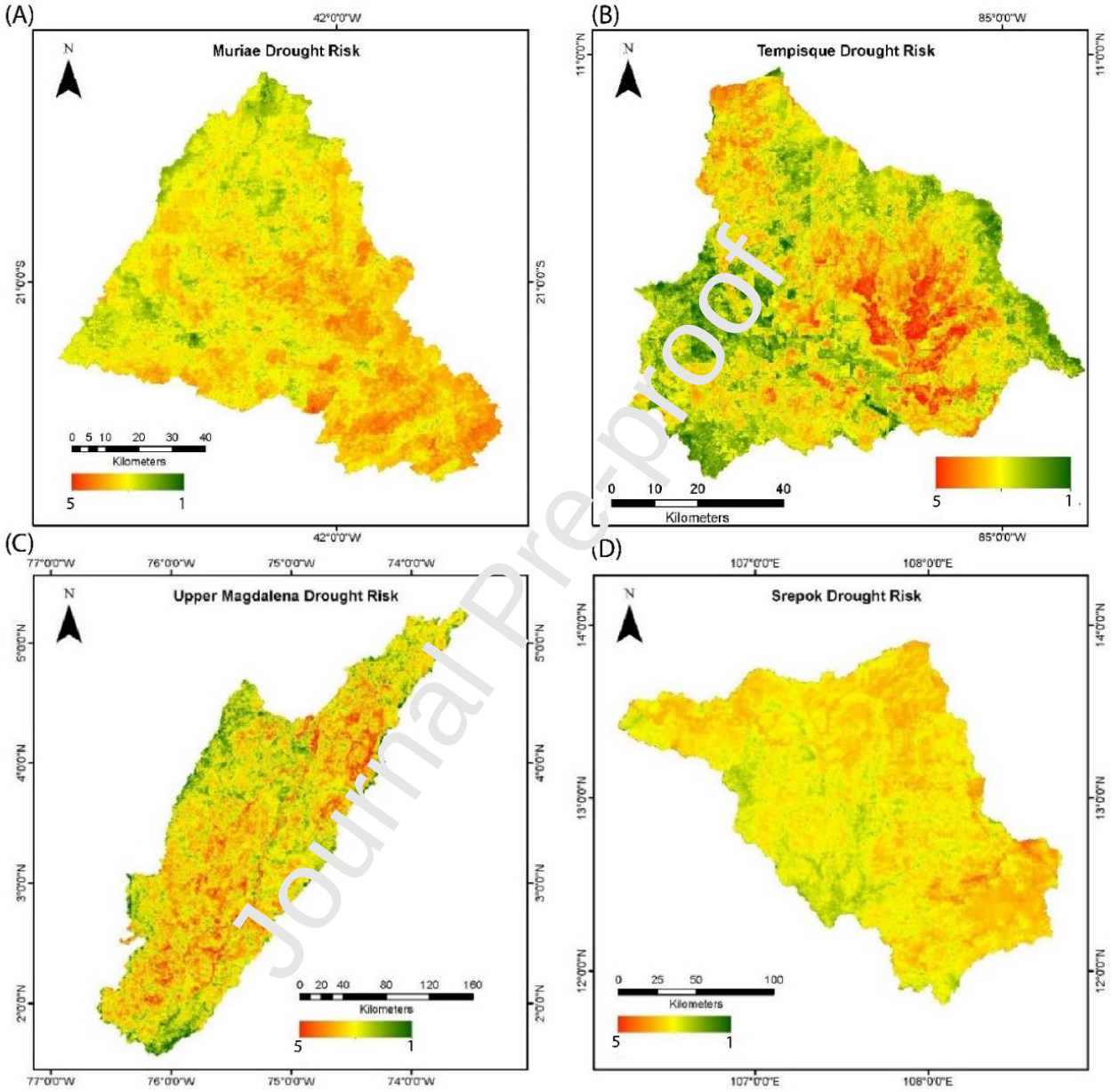

Figure 7: Map of severity class values for spatially distributed drought risk (*dr)* found in the four study regions

In all study regions, results show a considerable share of area with drought risk hotspots (with colours from orange to red). While in the **Muriaé,** highest risk was observed in the meteorologically drier downstream part, the **Tempisque** showed the strongest risk in the central-eastern and estuary region, where both

Journal Pre-proof

hazard and vulnerability values were found to be severe. For the **Upper Magdalena**, severe drought risk was found in the central Magdalena valley from up- to downstream (Northeast) and in the meteorologically drier Southeastern upstream part.

The **Srepok s**howed severe risk in the Southeastern Vietnamese upstream region and in the Northern and Eastern central region of Cambodia.

5 Discussion

5.1 Drought hazard (*dh*), drought vulnerability (*dv*) and drought risk (*dr*) in the four study regions - plausibility of identified drought risk hotspots

For the **Muriaé**, our results were able to display drought risk hotspots as well as the spatial distribution of severe drought hazard and vulnerability. Risk hotspots were found in the downstream area where most economic activities take place and precipitation rates are lower compared to those at higher elevations (CEIVAP, 2015; Nauditt et al., 2019b), along with a higher hydrological hazard also due to fractured geological and alluvial characteristics. Vulnerability is high all over the basin due to intensive livestock grazing and agricultural production as well as low GDP and large distances to road infrastructure. These spatial characteristics for drought hazard, vulnerability and risk were confirmed by collaborating stakeholders of the river basin committee CEIVAP (Comitê de Integração da Bacia Hidrográfica do Rio Paraíba do Sul) and the executive river basin agency AGEVAP (Agência da Bacia do Rio Paraíba do Sul). Additionally, results coincide with field research, modelling and data analysis related to spatial variability of drought occurrence and impacts of involved and affiliated scientists (Nauditt et al., 2019a).

Also the locations of drought risk hotspots in the **Tempisque** were well defined by the analysis. Hotspots were found in the Northwestern downstream part in the river estuary and in the Southeastern part along the main river stretches and the Bebedero tributary upstream. These regions show high values for both, hazard and vulnerability. Hazard is high due to human abstractions along the streams and irrigated areas and due to longer periods without rainfall and resulting vegetation moisture loss in the Eastern part of the basin. Risk hotspots (Figure 7) are found where this hazard is combined with highest vulnerability due to highest crop and livestock density. Lower drought risk (*dr)* values were found in the Northeast, where vulnerability is low in larger National Parks. The results are in agreement with information of the Water Agency of Costa Rica DA (Dirección de Agua de Costa Rica) and the team of the PIAAG Program (Programa Integral de

Abastecimiento de Agua para Guanacaste – Pacífico Norte) that aims at securing the water supply to the Tempisque Bebedero region (Dirección de Agua, 2018). These findings are supported by comprehensive (field) research in the drought prone study region on topics related to meteorological and hydrological droughts, water scarcity and vegetation susceptibility to droughts (Muñoz-Jiménez et al., 2019).

For the **Upper Magdalena Basin** in Colombia, drought risk hotspots were found in the Northeastern downstream part, all over the Magdalena valley and in the Southwestern upstream area (Figure 7). While agricultural activities and related water abstractions increase both vulnerability and hydrological hazard in the central valley, the risk hotspots in the upstream can be explained by strong meteorological hazard in the Southwest, which is drier and where most meteorological drought periods and vegetation related anomalies were detected. Hydrological droughts in the main stream are most probably aggravated by hydropower operation and abstractions for rice irrigation (Vega-Viviescas and Rodriguez, 2019). However, in total terms, the Upper Magdalena shows low total hazard in percentage of area with most values in Severity Class (*Sc*) 2 (52 %). This can be explained mainly by the few grid-cells affected by strong hydrological hazard along the major streams of the Magdalena. Vulnerability in the Magdalena was found to be more relevant compared to hazard with 43.1 % in *Sc* 4 and 55 % in *Sc* 3. This coincides with the spatial distribution of main areas of crop, livestock and population density in the Magdalena valleys and lower lying areas, as confirmed by scientists at Universidad Nacional de Colombia with vast research experience in the study region as well as by stakeholders as the Colombian Agency for Hydrology and Meteorology IDEAM and the Magdalena Basin Agency Cormagdalena.

Drought risk hotspots were also well detected in the **Srepok** basin, with main locations observed in the Southeastern upstream region over the Vietnamese highlands and the Cambodian North and Northwestern downstream region. High risk values depended mainly on high vegetation condition hazard (v_i) and hydrological hazard hh_{short} and hh_{long} that is dominating in the upstream area where reservoirs are located and along the downstream rivers, from where abstractions are used for irrigated rice in Cambodia (Bui Du, 2018; Constable, 2015). Vulnerability is lower compared to the other study regions, as approximately 50 % of the basin is covered with forest and due to the absence of livestock. Higher values for *dv* are only found in the Northwestern region, where agricultural land in Vietnam is cultivated with cash crops, mainly coffee (DaLat), rubber, cashew, black pepper and fruit trees for domestic and export markets (CCAFS-SEA). Results were confirmed by scientist of Aalto University with years of research experience in the region, as

well as by collaborating institutions (Ministry of Environment of Vietnam, MONRE and Water Management Institute NAWAPI).

5.2 Drought hazard assessment

In the **Muriaé**, severe hydrological hazard hh_{short_i} was found in the Northeastern agricultural upstream area, along the streams and at the river basin outlet with 20 % in severity class *Sc* 5 and another 20% in *Sc* 4. During the long-term drought in 2014-2015, the river stretch near the catchment outlet station fell dry (Nauditt et al., 2019b; Ribbe et al., 2018), with impacts on aquatic and riparian ecosystems and water users. This event was aggravated due to the fractured geological and alluvial characteristics of the downstream river bed (Nauditt et al., 2019b). Cumulative duration of hh_{long_i} with 12 or more days however, was only present in 14.1 % of area in *Sc* 4 and 1.8 % in *Sc* 5 at the aforementioned basin outlet. The Northeastern agricultural upstream area in Minas Gerais State is prone to hh_{short_i}, most probably due to smaller catchment areas and fast response to rainfall deficits.

Hydrostreamer provided excellent spatially distributed discharge simulations for the Muriaé catchment, as validated by station data and SWAT2012 modelling results for 93 stations; very valuable for drought and water resources management and planning. In the Southwestern downstream part severe meteorlogical hazard (*Sc 5)* was found for mh_{short_i}, mh_{long_i} for most grid cells. Low values were found for the upstream region (*Sc*1 for most grid cells). vc_i is following this spatial pattern with low hazard in the upstream and hazardous vegetation condition in the downstream area. This shows that not only the magnitude of rainfall in the mountainous upstream region (2000 m maximum elevation) was greater (Künne et al., 2018) compared to the drier downstream catchment, but also many less events with consecutive days without rainfall (mh_{short_i} and mh_{long_i}) occurred in the period between 1981 and 2018 (see individual index maps in the supplementary materials). Both regions are extremely vulnerable to meteorological droughts: while in the upstream part in Minas Gerais rainfed horticulture is dominating, downstream, in Italva, Rio de Janeiro State, livestock and milk production is the main economic activity (Fischer et al., 2018).

Hydrological drought hazard was found to be most severe along the upper streams of the **Tempisque** from which irrigation water is abstracted. This shows that our approach to assess hydrological hazard with a daily varying threshold is also suitable for anthropogenically intervened catchments, where human abstractions are leading to discharge anomalies – most probably increasing as a response to a

meteorological drought. 23.1 % of the basin area experienced more than 40 long drought events that lasted longer than 12 days (Q_{95} of daily varying discharge and below) and 10.5 % of its area was affected by 60 moderate drought events in the time period between 1918 and 2018. This shows the extreme low flows (down to 2.6 m³/s at Guardia station) the drought prone region is facing. A drought threshold of Q_{95} can therefore be considered as too low for a stream with a mean annual discharge of 27 m³/s in the case of the Guardia Station.

Strong spatial variation in meteorological drought hazard was found for mh_{short_i} and mh_{long_i}, with high values (*Sc* 5) covering the Eastern part of the basin (Bebedero subcatchment) and values of *Sc* 1-2 dominating the Western region (Tempisque). vc_i, in contrast, is homogeneously distributed all over the basin, probably as the NDVI image was taken during a dry anomaly (SPI -2) of a dry season. Although both total annual and dry season rainfall (December-May) accounts for similar monthly precipitation values in both regions (Bocanegra, 2017), results of our study show a much larger number of both short and long meteorological drought events in the Eastern Bebedero subcatchment compared to the Tempisque (see individual index maps in the supplementary materials)

In the **Upper Magdalena** only few grid-cell values for long and short hydrological hazard were identified along the major streams of the Magdalena. Hydrological droughts in the main streams are most probably aggravated by hydropower operation and abstractions for rice irrigation (Vega-Viviescas and Rodriguez, 2019). However, in total terms, the Upper Magdalena shows low hydrological hazard per percentage of area with most values in Severity Class (*Sc*) 2 (52%). This might be due to data uncertainties in the hydrostreamer results and the underlying observed discharge data (Rodríguez et al., 2020). Hydrostreamer yielded a poorer performance compared to the other three study regions.

The Southwestern upstream region showed strongest meteorological hazard (*Sc* 5) for mh_{short_i} and mh_{long_i} followed by the Northeastern downstream part and similar spatial patterns for vc_i. The Southwestern upstream region is exposed to a more marked tropical seasonality with two wet periods (April and May and October and November) and two long dry periods (June to October and November to April) (Rodríguez et al., 2020) while the lower part of the Magdalena receives more precipitation and is not exposed to such a marked seasonality.

For the **Srepok** basin, hydrological drought hazard for both hh_{long} and hh_{short} was found to be most severe in the Vietnamese Southern upstream region in the Vietnamese highlands due to discharge alterations

through hydropower operation, as well as in the Cambodian North-Central and Northwestern downstream region due to abstractions from agricultural activities.

Good results for Hydrostreamer downscaling results were obtained for the Srepok, being a study region of Kallio et al. (2019 & 2021), providing valuable discharge estimates for water resources modelling, management and planning in the transboundary basin and the Mekong region.

Meteorological hazard was strong with 55.9 % in *Scs* 4 and 5 for $mh_{long\ i}$, with all grid-cells located in the Vietnamese Southeastern upstream part. mh_{short_i} was only detected in Scs 1-3, indicating that periods without rainfall of shorter duration during the wet period were less frequent. vc_i, in contrast, is homogenously distributed all over the basin.

5.3 Vulnerability assessment

We applied open access gridded data sets to evaluate their suitability to provide drought vulnerability or exposure information for all of the four study regions. For all study regions, our indicator population density (p_i) showed few grid-cells with severity class values higher than *Sc 1* (classified as less than 50 persons per 1 km² grid-cell). This suggests that the classification we chose (Table 4), assuming that >50 persons would represent small settlements and agricultural communities in rural regions, might not be adequate. The number of persons per km² classified as vulnerable could be lower to also detect remote farmers. In contrast, low GDP in rural areas showed strongest severity (*Sc 5* = < 1 million USD PPP per km² for the reference year 2011) for almost all grid cells in all study regions, outweighing the low p_i values. We used this classification assuming a low GDP for rural agricultural regions; however, our results suggest that higher classification values for Severity classes *Sc 1* and *Sc 2* would be more adequate in order to display differences in GDP. In most risk studies, several exposure and vulnerability indicators are aggregated, regionally masked (Naumann et al., 2014, Carrão et al., 2016; Hagenlocher et al., 2019) to show overall vulnerability. Reference values for indicator classification – to the best of our knowledge – are not available in literature. Further research dealing with a detailed evaluation of gridded socioeconomic data in combination with a systematic approach for risk indicator classification, would be a valuable contribution to future comparative risk studies. Such a classification for different socioecological systems, as for example for tropical agricultural regions, could result in valuable classification reference values.

To evaluate drought exposure and vulnerability of agricultural activities, we tested the data set “Global Agricultural Lands in the Year 2000”. The resulting crop density evaluation, similarly as population density, is mostly distinguishing between grid cells with agriculture and no agricultural use; therefore, a low

classification values were used (Table 4) resulting in a good representation of agricultural exposure in the four study regions, as confirmed by affiliated scientists and stakeholders. More detailed local information on crop types, that would for example distinguish between perennial crash crops and annuals, irrigated or non-irrigated agriculture, could further detail such site-specific exposure information. Similarly as for Livestock density related vulnerability, we used a low number of animals grazing per grid cell to determine the low severity classes (S*c*s) (Table 4). Proximity to Infrastructure served as a good proxy for the stage of development of a location. Although drought vulnerability and exposure largely depends on storage infrastructure or irrigation systems, there are no available data sets for the regions addressed in this study. FAO AQUASTAT, for example, provides such data for Africa but not for Latin America and South East Asia. Despite these shortcomings, our overall drought vulnerability index *dv* showed good results for aggregated vulnerability. The Muriaé had most grid cells in high severity classes (73.1 % in *Sc 4*) due to its prevailing sectors milk production and agriculture as well as its sparse road infrastructure. For the Tempisque, we found fewer – but well distinguished and located – grid cells in severity class *Sc 4* (81.8 % in *Sc 3*); because of the existence of large National Parks in the Northeastern part, less livestock grazing and its well-developed road network. The Upper Mandarina, (with 43.1 % in *Sc4*) showed high drought vulnerability dv_i values in the downstream part mainly due to crop density and infrastructure. Only for the Srepok, less severe dv_i was found. This can be attributed to little livestock and crop density and larger forested areas compared to the other study regions. Strong dv_i was mainly found for the cultivated areas along the streams as in Vietnam (upstream Southeast), irrigated rice areas in the Cambodian Northeast, and in the downstream Northwest.

5.4 Limitations and further improvement

In summary, the main limitation to successfully implement our approach is the lack of available data, especially recent socioeconomic data at a high spatial resolution. Its accuracy depends on basin size in combination with the grid-cell size of the available data product. Our drought indices could be locally adapted by changing the severity classification (e.g. by increasing or reducing the duration of short and long droughts) or by introducing data sets that are not (yet) available for the regions addressed in this study. Furthermore, locally defined ecological flow and water demand thresholds could feed into a re-definition of local hydrological drought hazard indices. In addition, drought risk scenarios can be developed, helpful to detect potential changes in future drought risk. These could be based on hydro-climatic projections, indicating longer drought periods, or a changing vulnerability based on socioeconomic

projections. In its current state, our approach can deliver a presentation of spatially distributed drought hazard, vulnerability and risk hotspots in data scarce and rural tropical regions.

6 Conclusion

Droughts are causing severe damages to water abundant tropical countries worldwide. The implementation of drought adaptation measures at the local scale need to be based on reliable information about the spatially distributed drought risk -- that is rarely available in data scarce tropical catchments. We propose a methodology for evaluating and mapping the distribution of drought risk for rural tropical regions, based on the combination of independent indicators of daily data based drought hazard and drought vulnerability. We evaluated freely available gridded datasets regarding their suitability to assess drought hazard, vulnerability and risk in four differing rural tropical study regions, the Muriaé basin in South East Brazil, the Tempisque basin in Costa Rica, the upper catchment of the Magdalena basin, Colombia and the Srepok basin in Cambodia/Vietnam. We used daily scale meteorological and hydrological gridded data products and indices to evaluate tropical drought hazard, next to vegetation response to long term droughts, as well as vulnerability data related to the major sectors population, agriculture, livestock, infrastructure and GDP that were available for Latin America and South East Asia. Results showed spatial distribution of hazard, vulnerability and risk over the four study regions, as confirmed by local stakeholders, field surveys as well as through research of the authors. The following outcomes can be highlighted:

- The hydrological drought index hh_i, based on daily time series and a daily varying threshold Q_{95}, was able to detect hydrological drought hazard in both, pristine and regulated streams, representing both climate and human induced hydrological drought.
- The meteorological drought index mh_i, based on daily precipitation data and periods of zero rainfall turned out to be suitable for tropical regions as shown by local impacts especially on livestock and rainfed agricultural production;
- The subindices mh_{short_i} and mh_{long_i} and hh_{short_i} and hh_{long_i} give insights in the historical frequency of long and short drought events, independent of general seasonal patterns.
- In combination with the above-described findings, the vegetation anomaly response (NDVI/VCI) to longterm drought periods (SPI 12) reveals further vegetation, soil and groundwater related hazard, relevant for eg. forest fire related hazard.

- In light of the data scarcity in many tropical regions, the vulnerability related data sets and indicators related to crop and livestock density as well proximity to infrastructure have an adequate spatial resolution to provide vulnerability information at the local scale.
- The individual hazard and vulnerability indicator results give insights on how the classifications can be further adapted to individual study regions, depending on climate, topography, seasonality and human influence.
- Drought hazard, vulnerability and risk maps and individual indicator maps provide decision support when selecting and designing drought adaptation measures to avoid future drought impacts.

These findings were discussed with representatives of local universities and public institutions working in the study regions, by looking at each indicator and combined hazard, vulnerability and risk.

Our methodological framework offers a holistic, science based and novel solution to generate local drought risk knowledge that can feed into future drought related research. We recommend the replication of the approach in other tropical regions by using the developed R scripts. The outcomes produced are a valuable source of information for regional planners and water managers that take decisions on infrastructural and drought adaptation measures.

7 Acknowledgements

Field work scholarships, stakeholder workshops and travelling costs were supported by the CNRD Network Project (www.cnrd.info) and the Tropiseca project (https://www.researchgate.net/project/TROPISECA-Multi-lateral-University-Cooperation-on-the-Management-of-Droughts-in-Tropical-Catchments) funded by the German Federal Ministry of International Cooperation (BMZ)/German Academic Exchange Service (DAAD).

Journal Pre-proof

8 References

Adamson, P. and Bird, J., 2010: The Mekong: A Drought-prone Tropical Environment? International Journal of Water Resources Development, 26, 579–594, https://doi.org/10.1080/07900627.2010.519632.

AghaKouchak, A., Farahmand, A., Melton, F. S., Teixeira, J., Anderson, M. C., Wardlow, B. D., and Hain, C. R., 2015: Remote sensing of drought: Progress, challenges and opportunities, Rev. Geophys., 53, 452–480, https://doi.org/10.1002/2014RG000456.

AghaKouchak, A., Van Loon, A. F., Di Baldassarre, G., Breinl, K., Kuil, L., Garcia, M., Wanders, N., van Oel, P. R., Rangecroft, S., and Veldkamp, T. I. E., 2018: Water shortages worsened by reservoir effects, Nat Sustain, 1, 617–622, https://doi.org/10.1038/s41893-018-0159-0.

ANA, 2019: Portal HidroWeb, available at: http://www.snirh.gov.br/hidrotelemetria/Mapa.aspx, last access: 17 July 2019.

Arino, O., Ramos Perez, J. J., Kalogirou, V., Bontemps, S., Defourny, P., and van Bogaert, E., 2012: Global Land Cover Map for 2009 (GlobCover 2009), PANGAEA - Data Publisher for Earth & Environmental Science, https://doi.org/10.1594/PANGAEA.787668.

Ault, T. R., 2020: On the essentials of drought in a changing climate. Science, 368(6488), 256–260. doi:10.1126/science.aaz5492

AYA, 2019: Instituto Costarricense de Acueductos y Alcantarillados UEN de Gestión Ambiental Dirección de Estudios Básicos, available at: https://www.aya.go.cr/SitePages/Principal.aspx, last access: June 2019.

Bachmair, S., Svensson, C., Hannaford, J., Barker, L. J., and Stahl, K., 2016: A quantitative analysis to objectively appraise drought indicators and model drought impacts, Hydrol. Earth Syst. Sci., 20, 2589–2609, https://doi.org/10.5194/hess-20-2589-2016.

Baez-Villanueva, O. M., Zambrano-Bigiarini, M., Ribbe, L., Nauditt, A., Giraldo-Osorio, J. D., and Thinh, N. X., 2018: Temporal and spatial evaluation of satellite rainfall estimates over different regions in Latin-America, Atmospheric Research, 213, 34–50, https://doi.org/10.1016/j.atmosres.2018.05.011.

Baez-Villanueva, O. M., Zambrano-Bigiarini, M., Beck, H. E., McNamara, I., Ribbe, L., Nauditt, A., Birkel, C., Verbist, K., Giraldo-Osorio, J.D. & Thinh, N. X.: RF-MEP: A novel Random Forest method for

merging gridded precipitation products and ground-based measurements. Remote Sensing of Environment, 239, 111606. https://doi.org/10.1016/j.rse.2019.111606.

Beck, H. E., van Dijk, A. I. J. M., Roo, A. de, Miralles, D. G., McVicar, T. R., Schellekens, J., and Bruijnzeel, L. A., 2016: Global-scale regionalization of hydrologic model parameters, Water Resour. Res., 52, 3599–3622, https://doi.org/10.1002/2015WR018247.

Blauhut, V., Stahl, K., Stagge, J. H., Tallaksen, L. M., Stefano, L. de, and Vogt, J., 2016: Estimating drought risk across Europe from reported drought impacts, drought indices, and vulnerability factors, Hydrol. Earth Syst. Sci., 20, 2779–2800, https://doi.org/10.5194/hess-20-2779-2016.

Bocanegra, J. L., 2017: Hydrological drought assessment in the Tempisque-Bebedero catchment system in Costa Rica, Master, available at: https://epb.bibl.th-koeln.de/frontdoor/deliver/index/docId/1066/file/Thesis-Version+final-Bocanegra1.pdf.

Bui Du, D., 2018: Full Technical Report: Climate Change Impacts to Water Safety in the Greater Mekong region: D422Lot1.SMHI.5.1.1B: Detailed workflows of each case-study on how to use the CDS for CII production and climate adaptation, available at: https://climate.copernicus.eu/sites/default/files/2019-02/NAWAPI_Technical_report.pdf.

Cai, W., Borlace, S., Lengaigne, M. et al., 2014. Increasing frequency of extreme El Niño events due to greenhouse warming. Nature Climate Change, 4, 111–116. doi: 10.1038/nclimate2100

Cai, W., McPhaden, M. J., Grimm, A. M., Rodrigues, R. R., Taschetto, A. S., Garreaud, R. D., Vera, C., 2020. Climate impacts of the El Niño–Southern Oscillation on South America. Nature Reviews Earth & Environment, 1(4), 215–231. doi:10.1038/s43017-020-0040-3

Carrão, H., Naumann, G., and Barbosa, P., 2016: Mapping global patterns of drought risk: An empirical framework based on sub-national estimates of hazard, exposure and vulnerability, Global Environmental Change, 39, 108–124, https://doi.org/10.1016/j.gloenvcha.2016.04.012.

CCAFS-SEA, 2016: CGIAR Research Program on Climate Change, Agriculture and Food Security-Southeast Asia: Assessment Report: The drought crisis in the Central Highlands of Vietnam, available at: https://cgspace.cgiar.org/bitstream/handle/10568/75635/CGIAR%20ASSESSMENT%20REPORT_CentralH_June2.pdf.

CEIVAP, 2015: Sistema de Informações Geográficas e Geoambientais da Bacia Hidrográfica do Rio Paraíba do Sul, available at: http://sigaceivap.org.br/saibaMais, last access: 5 June 2019.

CIESIN, 2016: Gridded Population of the World (GPWv4) SEDAC, Columbia University, population density. http://doi.org/10.7927/H4NP22DQ. https://sedac.ciesin.columbia.edu/data/collection/gpw-v4, last access: 27.10.2020, 1997-2020.

Constable, D., 2015: The Sesan and Sre Pok River Basins, Bangokok, Thailand, 65 pp., available at: http://www.iucn.org/about/union/secretariat/offices/asia/regional activities/bridge 3s/, last access: 7 December 2018.

De Stefano, L., González-Tánago, I., Ballesteros, M., Urquijo, J., Blauhut, V., James, H., and Stahl, K., 2015: Methodological approach considering different factors influencing vulnerability – pan-European scale, Drought R&SPI, Technical Report no. 26, https://www.researchgate.net/publication/274536771_METHODOLOGICAL_APPROACH_CONSIDERING_DIFFERENT_FACTORS_INFLUENCING_VULNERABILITY__PAN-EUROPEAN_SCALE

Dirección de Agua, 2018: Programa Integral del Abastecimiento de Agua, available at: http://www.da.go.cr/wp-content/uploads/2018/04/Informe-Final_PIAAG-Version-Ditigal-Abril-2018.pdf,, last access: April 2019.

Dutta, T., Sharma, S., McRae, B. H., Roy, P. S., and DeFries, R., 2016: Connecting the dots: mapping habitat connectivity for tigers in central India, Reg Environ Change, 16, 53–67, https://doi.org/10.1007/s10113-015-0877-2.

Erfanian, A., Wang, G., and Fomenko, L., 2017: Unprecedented drought over tropical South America in 2016: significantly under-predicted by tropical SST, Nature Scientific reports, 7, 5811, https://doi.org/10.1038/s41598-017-05373-2.

European Commission, Joint Research Centre (JRC); Columbia University, Center for International Earth Science Information Network - CIESIN (2015): GHS population grid, derived from GPW4, multitemporal (1975, 1990, 2000, 2015). European Commission, Joint Research Centre (JRC) [Dataset] PID: http://data.europa.eu/89h/jrc-ghsl-ghs_pop_gpw4_globe_r2015a. Accessed through PREPdata, [01.11.2021]. www.prepdata.org.

FAO, 2019: Colombia: resilience programme 2017 - 2020, Rome, 24 pp., available at: http://www.fao.org/3/a-i7584e.pdf, last access: 27 June 2019.

Firoz, A. B. M., Nauditt, A., Fink, M., and Ribbe, L., 2018: Quantifying human impacts on hydrological drought using a combined modelling approach in a tropical river basin in central Vietnam, Hydrol. Earth Syst. Sci., 22, 547–565, https://doi.org/10.5194/hess-22-547-2018.

Fischer, S. B., Pedraza Luengas, A., Schlüter, S., and Oliveira Antunes, L. A. (Eds.) 2018: From design to implementation: a participatory appraisal for silvopastoral systems.: In: Nehren U, Schlüter S, Raedig C, Sattler D, Hissa H (Eds.), Strategies and tools for a sustainable rural Rio de Janeiro. ISBN 978-3-319-89644-1, Springer Series on Environmental Management, Springer International Publishing, Cham.

Fleig, A. K., Tallaksen, L. M., Hisdal, H., and Demuth, S., 2006: A global evaluation of streamflow drought characteristics, Hydrol. Earth Syst. Sci., 10, 535–552, https://doi.org/10.5194/hess-10-535-2006.

Fleig, A. K., 2004: Hydrological Drought – A comparative study using daily discharge series from around the world, Diplomarbeit, Freiburg, available at: http://www.hydrology.uni-freiburg.de/abschluss/Fleig_A_2004_DA.pdf, last access: 20 May 2019, 2004.

Funk, C., Peterson, P., Landsfeld, M., Pedreros, D., Verdin, J., Shukla, S., Husak, G., Rowland, J., Harrison, L., Hoell, A., and Michaelsen, J., 2015: The climate hazards infrared precipitation with stations--a new environmental record for monitoring extremes, Scientific data, 2, 150066, https://doi.org/10.1038/sdata.2015.66

González-Tánago, I., Urquijo, J., Blauhut, V., Villarroya, F., and De Stefano, L., 2015: Learning from experience: a systematic review of assessments of vulnerability to drought, Nat. Hazards, 80, 951–973, doi:10.1007/s11069-015-2006-1.

Gosling, S. N., Zaherpour, J., Mount, N. J., Hattermann, F. F., Dankers, R., Arheimer, B., Breuer, L., Ding, J., Haddeland, I., Kumar, R., Kundu, D., Liu, J., van Griensven, A., Veldkamp, T. I. E., Vetter, T., Wang, X., and Zhang, X., 2017: A comparison of changes in river runoff from multiple global and catchment-scale hydrological models under global warming scenarios of 1 °C, 2 °C and 3 °C, Climatic Change, 141, 577–595, https://doi.org/10.1007/s10584-016-1773-3.

Grimm, A. M. & Tedeschi, R. G., 2009. ENSO and extreme rainfall events in South America. Journal of Climate, 22, 1589–1609. doi:10.1175/2008JCLI2429.1

Journal Pre-proof

Hagenlocher, M., Meza, I., Anderson, C. C., Min, A., Renaud, F. G., Walz, Y., Siebert, S., and Sebesvari, Z., 2019: Drought vulnerability and risk assessments: state of the art, persistent gaps, and research agenda, Environ. Res. Lett., 14, 83002, https://doi.org/10.1088/1748-9326/ab225d.

Herrera, D. and Ault, T., 2017: Insights from a New High-Resolution Drought Atlas for the Caribbean Spanning 1950–2016, Journal of Climate, 30, 7801–7825, https://doi.org/10.1175/JCLI-D-16-0838.1.

Heydari, H., Valadan Zoej, M., Maghsoudi, Y., and Dehnavi, S., 2018: An investigation of drought prediction using various remote-sensing vegetation indices for different time spans, International Journal of Remote Sensing, 39, 1871–1889, https://doi.org/10.1080/01431161.2017.1416696.

Hoyos, N., Correa-Metrio, A., Sisa, A., Ramos-Fabiel, M. A., Espinosa, J. M., Restrepo, J. C., and Escobar, J., 2017: The environmental envelope of fires in the Colombian Caribbean, Applied Geography, 84, 42–54, https://doi.org/10.1016/j.apgeog.2017.05.001.

Hund, S. V., Grossmann, I., Steyn, D. G., Allen, D. M., & Johnson, M. S., 2021. Changing water resources under El Niño, climate change, and growing water demands in seasonally dry tropical watersheds. Water Resources Research, 57, e2020WR028535. doi:10.1029/2020WR028535

ICE, 2019: Instituto Costaricense de Electricidad: Instituto de Hidrologia, Costa Rica, available at: https://www.grupoice.com/wps/portal, last access: June 2019.

IDEAM, 2019: Observatorio del sistema de información del recurso hídrico: Sistema de Información Ambiental de Colombia, http://sirh.ideam.gov.co:8230/Sirh/faces/observatorio. jspx, last access: 4 May 2018.

IDEAM, PNUD, Alcaldía de Bogotá, Gobernación de Cundinamarca, CAR, Corpoguavio, Instituto Alexander von Humboldt, Parques Nacionales Naturales de Colombia, MADS, and DNP, 2014: Estrategia regional de mitigación y adaptación al cambio climático para Bogotá y Cundinamarca. Plan Regional Integral de Cambio Climático para Bogotá Cundinamarca (PRICC), available at: http://www.ideam.gov.co/documents/40860/609198/Policy+paper_07_Mitigaci%C3%B3n+y+adaptaci%C3%B3n+al+cambio+clim%C3%A1tico.pdf, last access: January 2019.

IPCC Climate Change, 2014: Impacts, Adaptation, and Vulnerability. Part B: Regional Aspects. Contribution of Working Group II to the Fifth Assessment Report of the Intergovernmental Panel on Climate Change https://www.ipcc.ch/report/ar5/wg2/.

Julien, Y., and J. A. Sobrino, 2009: The Yearly Land Cover Dynamics (YLCD) method: An analysis of global vegetation from NDVI and LST parameters. Remote Sens. Environ., 113, 329–334, https://doi:10.1016/j.rse.2008.09.016.

Kallio, M., Guillaume, J. H. A., Kummu, M., and Virrantaus, K., 2018: Generating improved estimates of streamflow using model averaging of downscaled runoff products under uncertainty, https://doi.org/10.13140/RG.2.2.33813.78562.

Kallio, M., Virkki, V., Guillaume, J. H. A., and van Dijk, A. I. J. M., 2019: Downscaling runoff products using areal interpolation: a combined pycnophylactic-dasymetric method, in El Sawah, S. (ed.) MODSIM2019: 23rd International Congress on Modelling and Simulation, https://doi.org/10.36334/modsim.2019.K8.kallio, available at: https://research.aalto.fi/files/39776673/kallio_et_al_MODSIM_201.).pdf.

Kallio, M., Guillaume, J. H. A., Virkki, V., Kummu, M., and Virrantaus, K., 2021: Hydrostreamer v1.0 - improved streamflow predictions for local applications from an ensemble of downscaled global runoff products. Geoscientific Model Development, https://doi.org/10.5194/gmd-14-5155-2021.

Kallio, M., 2020: Vignette Hydrostreamer, available at: https://github.com/mkkallio/hydrostreamer/tree/master/vignettes.

Karnieli, A., Agam, N., Pinker, R.T., Anderson, M., Imhoff, M.L., Gutman, G.G., Panov, N. and Goldberg, A., 2010: Use of NDVI and land surface temperature for drought assessment: Merits and limitations. Journal of climate, 23(3), 618-633, https://10.1175/2009/JCLI2900.1.

Karnieli, A., M. Bayasgalan, Y. Bayarjargal, N. Agam, S. Khudulmur, and C. J. Tucker, 2006: Comments on the use of the vegetation health index over Mongolia. Int. J. Remote Sens., 27, 2017– 2024. https://doi.org/10.1080/01431160500121727.

Kogan, F. N., 1995: Application of vegetation index and brightness temperature for drought detection, Advances in Space Research, 15, 91–100, https://doi.org/10.1016/0273-1177(95)00079-T.

Kummu, M., Taka, M., and Guillaume, J. H. A., 2018: Gridded global datasets for Gross Domestic Product and Human Development Index over 1990-2015, Nature Scientific data, 5, 180004, https://doi.org/10.1038/sdata.2018.4.

Mariano, D. A., Santos, C. A.C. d., Wardlow, B. D., Anderson, M. C., Schiltmeyer, A. V., Tadesse, T., and Svoboda, M. D., 2018: Use of remote sensing indicators to assess effects of drought and human-

induced land degradation on ecosystem health in Northeastern Brazil, Remote Sensing of Environment, 213, 129–143, https://doi.org/10.1016/j.rse.2018.04.048.

McKee, T. B., Nolan, D. J., and Kleist, J., 1993: The Relationship of drought frequency and duration to time scale, available at: https://climate.colostate.edu/pdfs/relationshipofdroughtfrequency.pdf.

Meza, I., Hagenlocher, M., Naumann, G., Vogt, J., and Frischen, J., 2018: Drought vulnerability indicators for global-scale drought risk assessments: Global expert survey results report, JRC technical reports, Publications Office of the European Union, Luxembourg, 62 pp., available at: https://collections.unu.edu/eserv/UNU:7430/Meza_etal_2019_DroughtVulnerability_META.pdf, 2019.MRC: Data and Information Services, available at: https://portal.mrcmekong.org/home, last access: 1 March 2019.

Muñoz Jiménez, R., Giraldo Osorio, J. D., Brenes Torres, A., Avendaño Flores, I., Nauditt, A., Hidalgo León, H. G., and Birkel, C., 2019: Spatial and temporal patterns, trends and teleconnection of cumulative rainfall deficits across Central America, Int J Climatol, 39, 1940–1953, https://doi.org/10.1002/joc.5925.

Nauditt, A., Hann, H.: Formiga, R., Ribbe, L., 2019a: Avaliação do risco de seca em uma bacia hidrográfica rural com escassez de dados: o caso da sub-bacia do rio Muriaé. In: Filho, A. et al (Eds.): Adapta Gestão Adaptativa do Risco Climático de Seca, UFC book series., available at: http://www.adapta.ufc.br/livro_adapta.pdf.

Nauditt, A.; Firoz, ABM; Viet, T. Q.; Fink, M.; Stolpe, H.; and Ribbe, L., 2017: Hydrological drought risk assessment in an anthropogenically impacted tropical catchment, in: Land Use and Climate Change Interactions in Central Vietnam: LUCCi, Nauditt, A., and Ribbe, L. (Eds.), Springer Book Series: Water Resources and Development, ISBN 978-981-10-2623-2.

Nauditt, A., Metzke, D., Thurner, J., Ribbe, L., Formiga-Johnsson, R. M., and de Paula Marques, A. L., 2019b: A grande seca de 2014-2015 Na Bacia Do Rio Paraíba Do Sul: Compreendendo As Características Espaciais E Temporais De Seca E Escassez Hídrica. In: Filho, A. Et Al (Eds): Adapta Gestão Adaptativa Do Risco Climático De Seca, Ufc Book Series., available at: http://www.adapta.ufc.br/livro_adapta.pdf.

Naumann, G., Barbosa, P., Garrote, L., Iglesias, A., Vogt, J., 2014: Exploring drought vulnerability in Africa: an indicator based analysis to be used in early warning systems. Hydrol. Earth Syst. Sci. 18, 1591–1604.

Naumann, G., Alfieri, L., Wyser, K., Mentaschi, L., Betts, R. A., Carrao, H., Spinoni, J., Vogt, J., and Feyen, L., 2018: Global Changes in Drought Conditions Under Different Levels of Warming, Geophys. Res. Lett., 45, 3285–3296, https://doi.org/10.1002/2017GL076521.

Naumann, G., Vargas, W., Barbosa, P., Blauhut, V., Spinoni, J., and Vogt, J., 2019: Dynamics of Socioeconomic Exposure, Vulnerability and Impacts of Recent Droughts in Argentina, Geosciences, 9, 39, https://doi.org/10.3390/geosciences9010039.

Neitsch, S. L., Arnold, J. G., Kiniry, J. R., and Williams, J. R., 2011: Soil and Water Assessment Tool Theoretical Documentation Version 2009.: Texas (Texas Water Resources Institute Technical Report, 406), available at: https://swat.tamu.edu/media/99192/swat2009-theory.pdf.

Nemani, R., and S. Running, 1989: Estimation of regional surface resistance to evapotranspiration from NDVI and thermal-IR AVHRR data. J. Appl. Meteor., 28, 276–284, https://doi.org/10.1175/1520-0450(1989)028<0276:EORSRT>2.0.CO;2.

Peel, M. C., Finlayson, B. L., and McMahon, T. A., 2007: Updated world map of the Köppen-Geiger climate classification, Hydrol. Earth Syst. Sci., 11, 1633–1644, https://doi.org/10.5194/hess-11-1633-2007.

Pinzon, J. and Tucker, C., 2014: A Non-Stationary 1981–2012 AVHRR NDVI3g Time Series, Remote Sensing, 6, 6929–6960, https://doi.org/10.3390/rs6086929.

Quiring, S. M. and Ganesh, S., 2010: Evaluating the utility of the Vegetation Condition Index (VCI) for monitoring meteorological drought in Texas, Agricultural and Forest Meteorology, 150, 330–339, https://doi.org/10.1016/j.agrformet.2009.11.015.

Räsänen, T. A., Lindgren, V., Guillaume, J. H. A., Buckley, B. M., & Kummu, M., 2016. On the spatial and temporal variability of ENSO precipitation and drought teleconnection in mainland Southeast Asia. Climate of the Past, 12(9), 1889–1905. doi:10.5194/cp-12-1889-2016

Ramankutty, N., Evan, A. T., Monfreda, C., and Foley, J. A., 2008: Farming the planet: 1. Geographic distribution of global agricultural lands in the year 2000, Global Biogeochem. Cycles, 22, n/a-n/a, https://doi.org/10.1029/2007GB002952.

Recuero, L., Litago, J., Pinzón, J. E., Huesca, M., Moyano, M. C., and Palacios-Orueta, A., 2019: Mapping Periodic Patterns of Global Vegetation Based on Spectral Analysis of NDVI Time Series, Remote Sensing, 11, 2497, https://doi.org/10.3390/rs11212497.

Journal Pre-proof

Ribbe, L., Formiga-Johnsson, R. M., and Ramirez Duval, J. L., 2018: Water Security in Rio de Janeiro State, In: Nehren U, Schlüter S, Raedig C, Sattler D, Hissa H (eds) Strategies and tools for a sustainable rural Rio de Janeiro. L. A., Springer International Publishing, Cham, 223–236, ISBN 978-3-319-89644-1, https://doi.org/10.1007/978-3-319-89644-1_15.

Robinson, T. P., Wint, G. R. W., Conchedda, G., van Boeckel, T. P., Ercoli, V., Palamara, E., Cinardi, G., D'Aietti, L., Hay, S. I., and Gilbert, M, 2014: Mapping the global distribution of livestock, PloS one, 9, e96084, https://doi.org/10.1371/journal.pone.0096084.

Rodríguez, E., Sánchez, I., Duque, N., Arboleda, P., Vega, C., Zamora, D., López, P., Kaune, A., Werner, M., García, C., and Burke, S., 2020: Combined Use of Local and Global Hydro Meteorological Data with Hydrological Models for Water Resources Management in the Magdalena - Cauca Macro Basin – Colombia, Water Resour Manage, 34, 2179–2199, https://doi.org/10.1007/s11269-019-02236-5.

Ruiz-Barradas, A., & Nigam, S., 2018. Hydroclimate Variability and Change over the Mekong River Basin: Modeling and Predictability and Policy Implications. Journal of Hydrometeorology, 19(5), 849–869. doi:10.1175/jhm-d-17-0195.1

Samaniego, L., Thober, S., Kumar, R., Wanders, N., Rakovec, O., Pan, M., Zink, M., Sheffield, J., Wood, E. F., and Marx, A., 2018: Anthropogenic warming exacerbates European soil moisture droughts, Nature Clim Change, 8, 421–426, https://doi.org/10.1038/s41558-018-0138-5.

Sheffield, J., Wood, E. F., Pan, M., Beck, H., Coccia, G., Serrat-Capdevila, A., and Verbist, K., 2018: Satellite Remote Sensing for Water Resources Management: Potential for Supporting Sustainable Development in Data-Poor Regions, Water Resour. Res., 54, 9724–9758, https://doi.org/10.1029/2017WR022437.

Smith, R. C. G., and B. J. Choudhury, 1991: Analysis of normalized difference and surface temperature observations over southeastern Australia. Int. J. Remote Sens., 12, 2021–2044, https://doi.org/10.1080/01431169108955234.

Stahl, K. and Hisdal, H., 2004: Hydroclimatology, in Tallaksen, L.M. and Van Lanen, H.A.J. (Eds.) Hydrological Drought., 2004. Developments in water science, 48, Elsevier, Amsterdam, 579p.

Stahl, K., Kohn, I., Blauhut, V., Urquijo, J., De Stefano, L., Acácio, V., Dias, S., Stagge, J. H., Tallaksen, L. M., Kampragou, E., Van Loon, A. F., Barker, L. J., Melsen, L. A., Bifulco, C., Musolino, D., de Carli, A., Massarutto, A., Assimacopoulos, D., and Van Lanen, H. A. J., 2016: Impacts of European drought

events: insights from an international database of text-based reports. Nat. Hazards Earth Syst. Sci., 16, 801–819, https://doi.org/10.5194/nhess-16-801-2016.

Stow, D. A., and Coauthors, 2004: Remote sensing of vegetation and land-cover change in Arctic tundra ecosystems. Remote Sens. Environ., 89, 281–308, https://doi:10.1016/j.rse.2003.10.018.

Sun, D., and M. Kafatos, 2007: Note on the NDVI-LST relationship and the use of temperature-related drought indices over North America. Geophys. Res. Lett., 34, L24406, https://doi:10.1029/2007GL031485.

Thirumalai, K., DiNezio, P. N., Okumura, Y., and Deser, C., 2017: Extreme temperatures in Southeast Asia caused by El Niño and worsened by global warming, Nature Communications, 8, 15531, https://doi.org/10.1038/ncomms15531.

Thomas, A. C., Reager, J. T., Famiglietti, J. S., and Rodell, M., 2014: A GRACE-based water storage deficit approach for hydrological drought characterization, Geophys. Res. Lett., 41, 1537–1545, https://doi.org/10.1002/2014GL059323.

Tijdeman, E. and Menzel, L., 2020: Controls on the development and persistence of soil moisture drought across Southwestern Germany, HESS preprint, https://doi.org/10.5194/hess-2020-307.

UNGRD, IDEAM, MinAmbiente, Cancillería de Colombia, and United Nations, 2018: Estrategia Nacional para la Gestión Integral de la Sequía en Colombia, available at: https://www.unisdr.org/files/11541_DroughtRiskReduction2009library.pdf.

UN-ISDR, 2009: Drought Risk Reduction, Framework and Practices: Contributing to the Implementation of the Hyogo Framework of Action, Geneva, 214 pp., available at: https://www.unisdr.org/files/11541_DroughtRiskReduction2009library.pdf, last access: 28 July 2019.

Van Wijk, M. T., M. Williams, J. A. Laundre, and G. R. Shaver, 2003: Interannual variability of plant phenology in tussock tundra: Modelling interactions of plant productivity, plant phenology, snowmelt and soil thaw. Global Change Biol., 9, 743–758, https://doi.org/10.1046/j.1365-2486.2003.00625.x.

Vega-Viviescas, C. and Rodriguez, E. A., 2019: Evaluation of reanalysis data in the study of meteorological and hydrological droughts in the Magdalena-Cauca river basin, Colombia, Dyna (Medellin, Colombia), 86, 268–277, available at: https://www.researchgate.net/publication/338456293_Evaluation_of_reanalysis_data_in_the_study_of_meteorological_and_hydrological_droughts_in_the_Magdalena-Cauca_river_basin_Colombia.

Venegas-Cordero, N., Birkel, C., Giraldo-Osorio, J. D., Correa-Barahona, A., Duran-Quesada, A. M., Arce-Mesen, R., and Nauditt, A., 2020: Can hydrological drought be efficiently predicted by conceptual rainfall-runoff models with global data products?: Accepted and under review at Journal of Natural Resources and Development.

Vogt, J.V., Naumann, G., Masante, D., Spinoni, J., Cammalleri, C., Erian, W., Pischke, F., Pulwarty, R., Barbosa, P., 2018; Drought Risk Assessment. A conceptual Framework. EUR 29464 EN, Publications Office of the European Union, Luxembourg, 2018. ISBN 978-92-79-97469-4, doi:10.2760/057223, JRC113937.

Walker, M. D. et al., 2006: Plant community responses to experimental warming across the tundra biome. Proc. Natl. Acad. Sci. USA, 103, 1342–1346, https://doi.org/10.1073/pnas.0503198103.

WMO, 2008: Manual on Low-flow – Estimation and Prediction: Operational Hydrology Report No. 50, Geneva, 138 pp., available at: https://www.wmo.int/pages/prog/hwrp/publications/low-flow_estimation_prediction/WMO%201029%20en.pdf, last access July 2021.

Journal Pre-proof

Graphical abstract

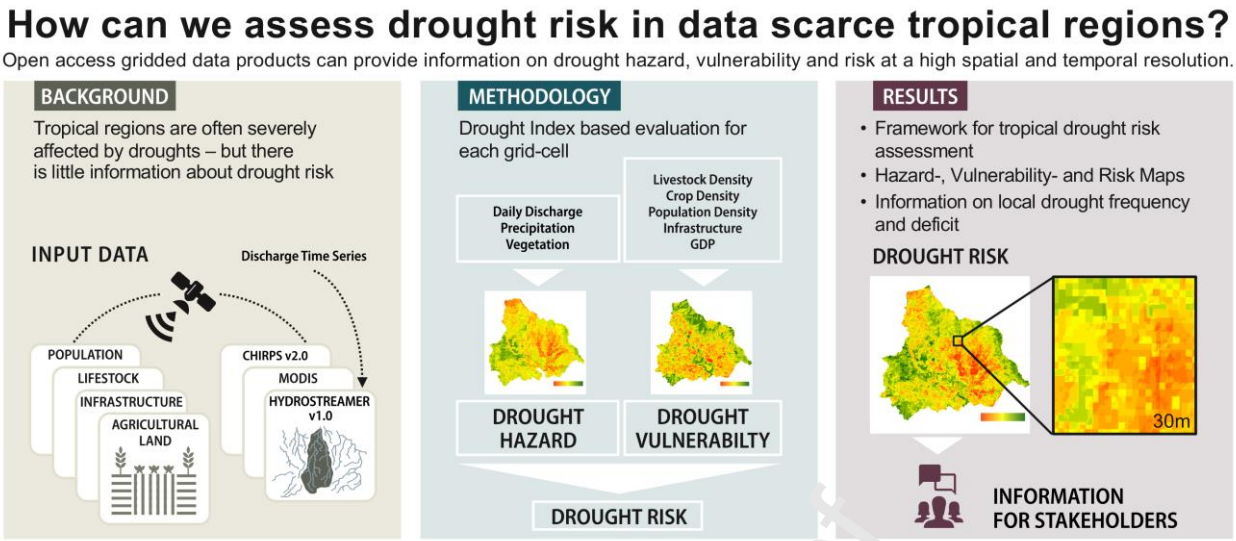

Journal Pre-proof

Highlights

- Droughts are strongly affecting tropical regions while research on tropical drought risk is sparse
- We evaluated hazard and vulnerability related gridded data sets for 4 contrasting tropical catchments
- Short term, daily data based drought indices are adequate, as tropical catchment systems have a quick hydrological response and little storage capacity.
- Frequency of short and long term meteorological and hydrological droughts using daily data
- Drought hazard, vulnerability and risk maps for drought adaptation

Journal Pre-proof

Declaration of interest Statement

The authors declare that they have no conflict of interest.

Journal Pre-proof

Declaration of interests

☒ The authors declare that they have no known competing financial interests or personal relationships that could have appeared to influence the work reported in this paper.

☐The authors declare the following financial interests/personal relationships which may be considered as potential competing interests:

Alexandra Nauditt on behalf of all the authors

Journal Pre-proof

Author contributions

Alexandra Nauditt conceived and designed the study and overall methodology, performed the analyses and prepared the manuscript. Kerstin Stahl contributed to the study design, methodology, manuscript writing and structure. Erasmo Rodriguez, Christian Birkel and Rosa Formiga and Marko Kallio supported field work, local validation of results and stakeholder communication in terms of research and information demand to support drought management and validation as well as the writing process. Marko Kallio simulated high spatial resolution discharge time series (hydrostreamer). Hamish Hann, Oscar Baez and Joschka Thurner supported the methodological setup, R Coding, Package for GitHub and Cran and development of illustrations (R Graph Gallery). Lars Ribbe supported and accompanied the research by allocating time and financial resources for personnel, travels and field work. All authors actively took part in the writing and editing process.

Journal Pre-proof